ANALYSIS OF SELF-SENSING CAPABILITIES OF GO AND rGO BASED CEMENTITIOUS COMPOSITES

A dissertation submitted in partial fulfilment of the requirement for the award of the degree of

MASTER OF

ENGINEERING

in

STRUCTURAL

ENGINEERING

Submitted by

AYUSH BHATIA

(802024033)

Under the supervision of

DR. SHRUTI SHARMA
Professor
Department of Civil Engineering
TIET, Patiala

DR. ARPIT GOYAL
Assistant Professor
Department of Civil Engineering
TIET, Patiala

DEPARTMENT OF CIVIL ENGINEERING

THAPAR INSTITUTE OF ENGINEERING AND TECHNOLOGY

(DEEMED TO BE UNIVERSITY)

PATIALA-147004 (PUNJAB)

AUGUST 2022

DECLARATION

I hereby declare that the work which is presented in this dissertation entitled **"Analysis of Self -Sensing capabilities of GO and rGO based cementitious composites"** as per the requirements for the award of **Master of Engineering** in **Structural Engineering**, submitted in the Department of Civil Engineering, Thapar Institute of Engineering and Technology (TIET), Patiala, is an authentic record of work. This work is carried out under the guidance of **Dr. Shruti Sharma** and **Dr. Arpit Goyal.** It is declared that this work is original and has not been submitted anywhere else for the award of any other degree or certificate.

Ayush Bhatia
802024033

Date: 30/8/2022

CERTIFICATE

This is to certify that the above declaration made by the student concerned is correct according to the best of my knowledge and belief.

DR. SHRUTI SHARMA
Professor
Department of Civil Engineering
TIET, Patiala

DR. ARPIT GOYAL
Assistant Professor
Department of Civil Engineering
TIET, Patiala

ACKNOWLEDGEMENT

This research thesis could not have been completed without the help and guidance of many people who contributed directly or indirectly through their constructive criticism. I wish to express my deep gratitude to **Dr. Shruti Sharma,** Professor, Department of Civil Engineering, Thapar Institute of Engineering and Technology, Patiala and **Dr. Arpit Goyal,** Assistant Professor at Department of Civil Engineering, Thapar Institute of Engineering and Technology, Patiala, for providing their guidance, support and patient listening to my ideas and also suggesting new ways for implementing my ideas. For the motivation and inspiration that triggered me throughout my work. I would also like to thank all the staff members at the Institute for providing all the help and facilities I required to complete the research. I do not find enough words which can express my feeling of thanks for their help in carrying out various experiments and procedures. Additionally, I would like to acknowledge the financial support provided by the Thapar Institute of Engineering & Technology from the seed grant project (Ref: TU/DORSP/1559) of Dr Arpit Goyal for the purchase of materials. Finally, I would like to dedicate this thesis to my family who has always been a great source of support and encouragement especially in all my academic endeavors.

Ayush Bhatia
802024033

ABSTRACT

The addition of steel and carbon fibers to a cementitious composite to lower the composite's resistivity and create a piezoresistive matrix has recently been used as an innovative method of detecting various structural states. As SHM sensors, smart cement-based nanomaterials of graphene derivatives like carbon fibre or carbon nanotube cementitious hybrids, or a mix of the two, are piezo-resistive, which means that resistivity varies with the given load/strain. This indicates that a cement sample or building does not require the external or additional attachment of any sensor. Instead, the cement composite is able to detect its own strain as well as several other factors.

The present study describes the various tests that have been done to evaluate the mechanical and electrical properties of cementitious mortar specimens with varying percentages of GO (Graphene Oxide) and rGO (Reduced Graphene Oxide). Testing has been done after 7, 28 and 56 days of curing. Mechanical properties included compressive strength test and flexural strength test, whereas, electrical properties included electrical resistivity test and piezo resistivity test. The piezoresistive action of functional filler particles, that are spread throughout the composite phase create a conductive connection, is what gives its self-sensing ability. As a result, anytime cementitious composite is forced in a certain way, the network changes, changing the electrical resistivity.

Results from various tests show that both GO and rGO increased the compressive strength and flexural strength of the cementitious mortar at 28 days and 56 days. On addition of GO and rGO at all addition percentages, FCR (Fractional Change in Resistivity) decreases on increasing the load, corresponding to increase in electrical conductivity and comes back to its original value after sample failure in monotonic loading, corresponding to decrease in conductivity. Thus, overall pattern of piezoresistive behaviour is followed. Compared to GO, in rGO specimens, cluster of rGO is more randomly distributed, this is attributed to lower surface area of rGO, compared to GO. It was found that rGO 0.06% achieved the maximum sensitivity, followed by GO 0.3%, indicating maximum contact points are formed in rGO 0.06% leading to enhanced piezoresistive behaviour. The piezoresistive performance of cementitious composites with GO and rGO confirms their ability to become intrinsic cement-based sensors.

TABLE OF CONTENTS

LIST OF FIGURES

LIST OF TABLES

CHAPTER 1
INTRODUCTION

1.1 GENERAL

The necessity to track and analyse concrete performance throughout maintenance or service life using condition evaluation technologies and varied materials has gotten increased attention over the years. Structural Health Monitoring (SHM) is a new technique that may detect any deficiencies in a structure's performance before it leads to a major loss of capacity (Kuang et al, 2009). The term "SHM" refers to a technology that continually assesses a structure's condition to identify developing defects and avoid collapse or failure. One of the best options is an early damage monitoring tool that may be used on the load-bearing structural system (Kuang et al, 2009). The most significant benefit is that an identified vulnerability can be assessed early on, and the harm may be repaired if necessary. SHM's goal is to correctly analyse a structure's functionality, continually monitoring its performance and delivering real-time data on its present state. The rate of corrosion, alkali reactions, humidity, ionic strength, loads, accelerations, strains, and fractures are some of the factors that may be monitored with SHM (Kuang et al, 2009).

The goal of structural health monitoring is to use a sensory system to continually and precisely measure the functioning of structures. Cement-based sensors, which were recently introduced, are piezoresistive and may thus be utilized to detect stress/strain directly by analysing their electrical resistance. Such sensors, commonly referred to as smart (self-sensing) structural composites, can be incorporated as a portion or entire structure, providing structural capabilities as well as a reaction to imposed stress and damage (Azhari & Banthia, 2012).

The capacity of cementitious materials containing conductive particles to self-sense for SHM has piqued interest in recent decades. Different materials and sensors have evolved, according to previous literature, but they are still not widely used in practice, because the materials used for the conductive phase can be highly expensive. It is difficult to disperse within the cementitious matrix, which is particularly the case for nanoscale materials like carbon nanotubes (CNTs) (Sun et al, 2010).

Electric-resistivity strain gauges, piezo-resistivity detectors, and optic sensors are employed extensively as sensors for assessment and monitoring in construction. However, their use has

significant disadvantages, such as limited sensitivity and poor durability. Technological improvements in smart materials, such as cement-based sensors, may be able to address these concerns. (Wang et al, 2015).

1.2 NANO-ENGINEERING IN CEMENTITIOUS COMPOSITES

Nano-engineering is a new discipline that is rapidly growing in popularity. The profession of nanoscale engineering encourages the technology of nanoscale structure manipulation to create a new generation of modified, multi-functional, multi-dimensional materials. Low electrical resistivity, self-sensing capabilities, self-cleaning, self-healing, excellent durability, and fracture control are all features of cementitious composites incorporating nanoparticles. (Banthia et al. 1992).

Nanotechnology is extremely important in the realm of study. Fullerenes, quantum dots, nanorods, nanotubes, and other nanomaterials are only a few examples. They are used as a cement mortar ingredient to improve strength and durability. As SHM sensors, smart cement-based nanomaterials are widely acknowledged. These carbon fibre or carbon nanotube cementitious hybrids, or a mix of the two, are piezo-resistive, which means that resistivity varies with the given load/strain. Because of their incredibly small dimensions, carbon fibres offer a highly efficient inter-fibre consistency and hence significantly increase the conductivity of cement mixtures (Banthia et al. 2012).

1.2.1 NANOMATERIALS USED IN CEMENTITIOUS COMPOSITES

Nanomaterials are more expensive than traditional materials, hence they are unlikely to be used in large-scale construction projects and also for research purposes (**Figure 1.1**). Mortar may be made into a versatile smart efficient material with the use of various kinds of nano-materials. These nano-materials serve to improve the pore structure, which improves the durability qualities. Various types of nanomaterials used in cementitious composites are as follows:

- **Nano Silica**- Silica nanoparticles made up of practically pure silica have a high specific surface area and a high proportion of very fine microscopic particles (99 percent). Properties of such a material are similar to those of silica fume, but they are enhanced due to a wider specific area, resulting in increased responsiveness. By occupying the gaps between fly ash and cement particles, nano-silica boosts the strength properties of concrete mixes containing substantial amounts of fly ash during an initial stage.
- **Carbon Nano-Fibres (CNFs)-** Carbon nanofibers (CNFs) are spherical nanostructures made up of graphene layers stacked in cones, cups, or plates with exceptional

mechanical characteristics and conductivity (both thermal & electrical). They are also known as Vapour Generated Carbon Fibres (VGCFs) or Vapour Grown Carbon Nanofibers (VGCNFs). The hollow core of each individual nano-particle is encircled by the cylindrical core (Sun et al, 2015).

- **Graphene oxide (GO)-** Graphene oxide (GO) is a one-of-a-kind substance that consists of a single monomolecular layer of graphite with epoxide, carbonyl, carboxyl, and hydroxyl groups. (Koh et al, 2014). GO is a delicate, unique & a very fascinating nanomaterial. The overall size of GO as an operationalized mono-atomic layer of carbon is around 1nm. The horizontal dimension of GO panels, on the other hand, can reach micrometres.
- **Reduced Graphene oxide (rGO)-** rGO is a form of graphene oxide that has undergone chemical, thermal, and other processing to reduce the oxygen amount. The oxygen content present in rGO ranges from 5-10% as compared to GO which has 15-32% oxygen content respectively. (Qureshi et al, 2019)
- **Carbon Nanotubes (CNTs)-** Carbon nanotubes are cylinder-shaped hollow graphene sheets having dual dimensionality in the nanoscale (Safiuddin et al., 2014). Chemically, electronically, mechanically, and optically, they are incredible. Being one of nanotechnology's most potential materials CNTs can be categorized into 2 types (**Figure 1.2**):
    a) Single-Walled CNTs
    b) Multi-Walled CNTs

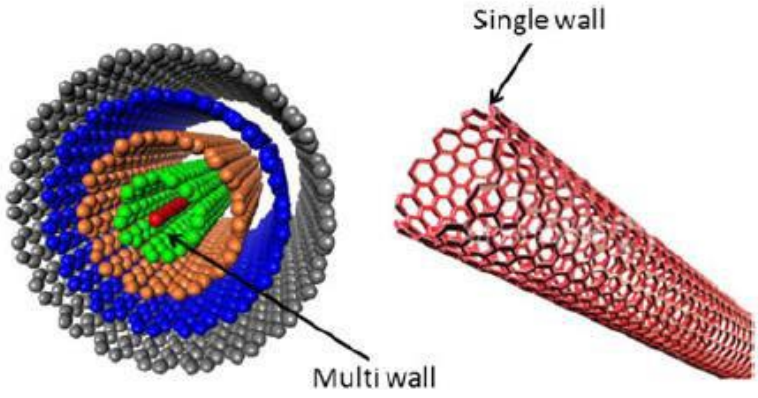

Figure 1.2 Single Walled and Multi-Walled CNTs, (Safiuddin et al., 2014).

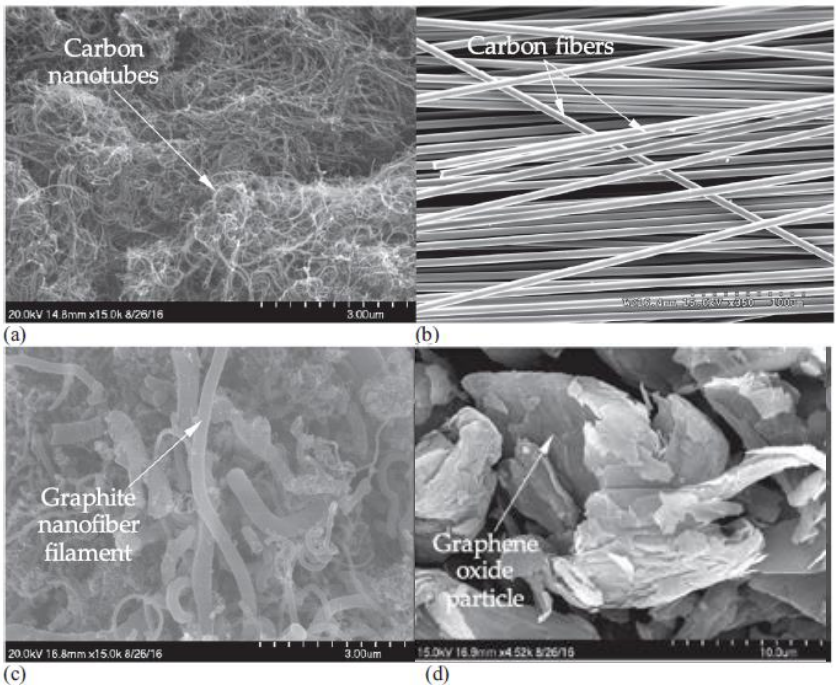

Figure 1.1 Geometrical shape of nanomaterials; (a) CNT, (b) CF, (c) GNF, (d) GO.

(Yoo et al, 2019)

1.3 GRAPHENE DERIVATIVES

Graphene is a single-layer crystal of carbon atoms, usually exfoliated from graphite. It has a honeycomb hexagonal lattice fabricated by sp2 hybridized bonds. The rhombic unit cell of single-layer graphene contains two carbon atoms A and B (**Figure 1.3**). The C-C distance is 0.142 nm (Huo, 2017). The graphene crystal is not a perfect 2D plane, but contains ripples around 1 nm in size. An endless 2D structure represents the perfect graphene. Armchair and zigzag edges stand out among the two main forms of edges. These two varieties of edges result in various electronic characteristics of graphene flakes (Huo, 2017).

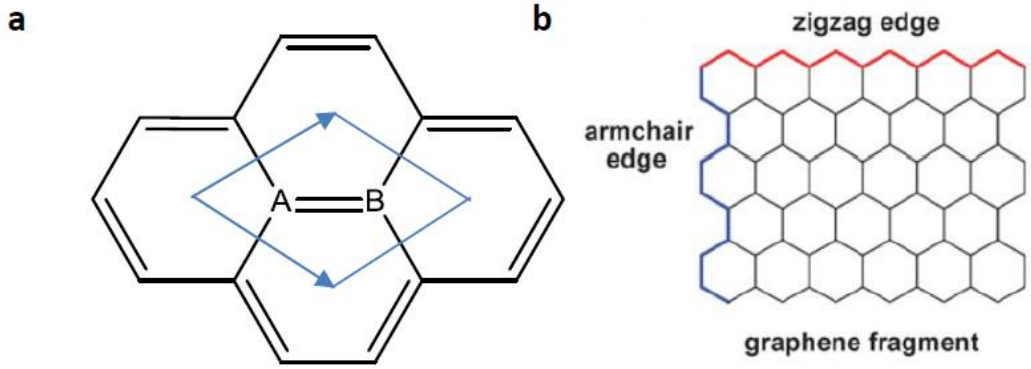

Figure 1.3 (a) Two carbon atoms A and B of unit-cell of graphene; (b) Two forms of edges in graphene flake: Zigzag and armchair. (Huo, 2017)

1.3.1 Graphene Oxide

Graphene oxide (GO) and graphene have structural similarities. Both of the products feature a hexagonal carbon matrix, but when it is connected to the oxygen - containing groups, the GO layer is often deformed (**Figure 1.4**). GO is a fluffy, very-light black powdered nanomaterial. GO has been investigated for years as a potential raw ingredient for commercially viable graphene synthesis. GO has a wide range of uses, including possible electrode materials for Li-ion batteries and clear conductors in organic solar cells (Koh et al, 2014). it is also used for water desalination and making anti-barrier coatings. Considering these sophisticated applications, the basic analysis of GO's structure has remained sluggish. Although several speculative theories for GO have been put out by researchers, there is still debate regarding its exact molecular composition (Raccichini et al, 2015). Sample-to-sample variation resulting from various synthesis procedures, the degree of oxidation, the quantity of amorphization, the non-stoichiometric nature of GO, and the weak resolution of the most important characterisation tools like Solid-state nuclear magnetic resonance (SSNMR) spectroscopy and Fourier transform infrared (FTIR) spectroscopy are some of the main causes (Raccichini et al, 2015).

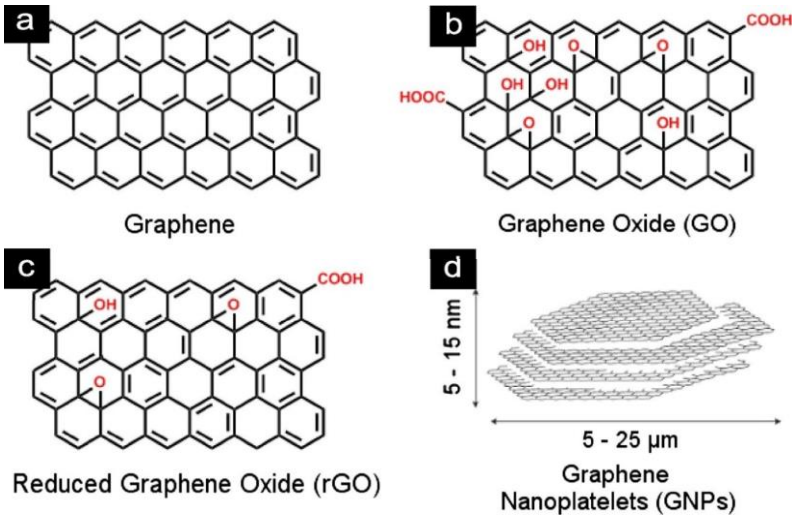

Figure 1.4 Chemical depiction of graphene along with its derivatives: (a) graphene, (b) graphene oxide, (c) reduced graphene oxide, (d) common sizes of graphene nanoplatelets.

(Koh et al, 2014)

1.3.2 Reduced Graphene Oxide

In contrast to graphene oxide, which is created when graphite is oxidised and results in enhanced interlayer positioning and functionalization of the basal planes of the substance, reduced graphene oxide (rGO) is a form of graphene oxide that has undergone chemical,

thermal, and other processing to reduce the oxygen amount (Koh et al, 2014).The oxygen content present in rGO ranges from 5-10% as compared to GO which has 15-32% oxygen content respectively (**Figure 1.4**). rGO can be used to make chemical sensors (Koh et al, 2014). rGO can be used for various applications such as it can be used for making anti-corrosion coatings by using such a small quantity of it. Also, very minute quantities of it by weight of cement can be used to enhance the mechanical and electrical properties of concrete (Qureshi 2020).

1.4 SELF SENSING CONCRETE

Self-Sensing Concrete (SSC) has received much research due to its potential to offer a practical and affordable answer for the structural health monitoring of civil infrastructure, making it particularly appealing for use in practical scenarios (Konkanovs et al, 2020). The piezoresistive action of functional filler particles, that are spread throughout the composite phase and create a conductive connection, is what gives concrete its self-sensing ability. As a result, anytime concrete is forced in a certain way, the network changes and changes the electrical resistivity (Konkanovs et al, 2020). Altogether, the self-sensing concrete has a highly complicated framework. The use of self-sensing concrete might enhance the safety, longevity, service life, and dependability of structural concrete by allowing them to detect and monitor them (Dong et al, 2019).

Carbon black (CB), Carbon fibres (CF), Graphite nanofibers (GNF) and carbon nanoparticles like carbon nanotubes (CNT) and carbon nanofiber (CNF) are examples of conductive functional fillers that are used in self-sensing concrete to attain its attributes (Faghih, 2018) Certain hybrids can also provide concrete various sensing capabilities that traditional fillers were unable to deliver. The cementing matrix and each of the conductive materials act as a conduit for the electricity, creating an electrical connection (Wen et al, 2007).

The specimen is often loaded under compression or tension to assess Fractional change in resistance (FCR) or the sensitivity of a cement-based sensor. The sensing behaviour of conductive components in a cement-based composite under pure compression or tension, can be assessed by various tests such as piezo resistivity measurement, electrical resistivity, conductivity etc. The capacity to sense strain under flexure is crucial since cement-based sensors must be used on bending structures like beams and bridge decks (Han et al, 2015).

1.1.1 Measurement of sensing signal of cement mortar composite

The sensitivity of the concrete may be determined by a variety of parameters, including piezo-resistivity, electrical resistivity, dielectric constant, conductivity, and capacitance (Han et al, 2015). However, one of the simplest techniques is the use of electrical resistance or resistivity as a sensitivity indicator. The electrical resistivity, which fluctuates with compression, temperature, or damage, is influenced by the fibre conductivity found inside cement-based composites. To evaluate electrical conductivity in various setups, electrodes constructed of suitable materials are utilized (Mo et al, 2013). Before selecting an electrode, three parameters (material, fixing placement, and pattern) should be taken into account. The material should have two major qualities: Low electrical resistance and stable conductive quality. These electrodes may be affixed to the composite's surface, inserted deep inside the composite, or positioned in a clipping pattern. Among these, embedding and attaching are two of the most popular techniques. Experiments can be performed using a two-probe method or even a four-probe set-up with both electrodes acting as the current pole and voltage pole (Dahawi et al, 2017).

In contrast to a two-probe method, the inner probes are employed to examine voltage while the outside probes serve as current detectors in a four-probe method. Comparing the two-probe approach to the four-probe method, the two-probe method is more practical and easier to apply (**Figure 1.5**). However, when low resistance values are measured using the four-probe approach, it is typically preferred due to the precision of the results (Han et al, 2015)

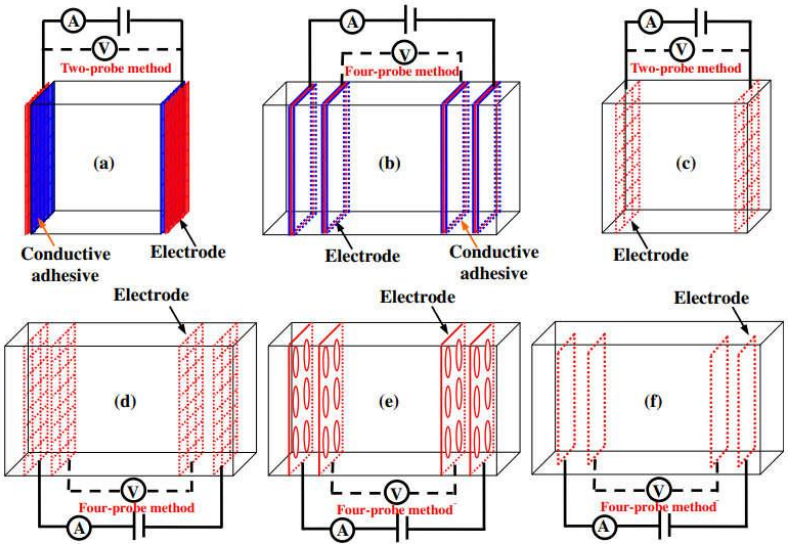

Figure 1.5 Fixing the style and layout of electrodes in self-sensing concrete; (a,b): electrodes attached on the surface; (c–f): embedded mesh, perforated plate or loop electrode. (Han et al, 2015).

1.4.2 Electrical Resistivity

Resistance is not only based on the substance's electrical characteristics. The dimensions of a conductor or specimen, such as its length, have an impact as well. This coherence may be compared between different materials independent of their form thanks to the electrical resistivity (Ωm), which is what gives this coherence its name.

Electrical resistivity is used as a measure of a material's electrical efficiency to make it more comparable to other materials based on their ability to conduct electricity, such as cementitious composites. **Equation 1.1** may be used to determine the resistivity as the resistance per unit length (Lee et al, 2017). Therefore, resistivity is a fundamental characteristic of resistance.

$$\rho = R\,\frac{A}{L} \tag{1.1}$$

Where A (m²) is the cross-sectional area and l (m) is the distance between two voltage electrodes.

The electrical conductivity σ (S/m), also known as specific conductance, is a measurement of a material's capacity to carry an electric current and is essentially the reciprocal of electrical resistivity. **Equation 1.2** can be used to express the conductivity in relation to resistivity.

$$\sigma = R\frac{L}{A} = \frac{1}{\rho} \tag{1.2}$$

1.4.3 Piezo-Resistivity

Piezo-resistivity is an electrical phenomenon that is defined as the shift in electrical resistivity caused by an applied compression. The strain in cementitious self-sensing composite materials is measured using this technique. The main technique involves measuring changes in electrical resistance in a conductor or specimen in addition to assessing material stress/strain, thus the specimen can act as a self-sensing strain-sensor (Chung, 2016).

Computing the Fractional Change in Resistivity (FCR) represents the stress/strain value in a piezo-resistive sensor. The ratio of the initial electrical resistivity to the change in electrical resistivity is known as the FCR (**Equation 1.3**). Given that its reaction is proportionate and reversible to the actual strain detected by a sensor, the FCR is therefore utilised as a stress/strain sensing indication (Lee et al., 2017).

$$FCR = \frac{\rho_1 - \rho_0}{\rho_0} = \frac{\Delta\rho}{\rho_0} = \frac{\Delta R}{R} \tag{1.3}$$

Where $\Delta\rho$ is the change in resistivity, ρ_1 the resistivity after applying stress/strain and ρ_0 the initial resistivity.

1.5 OBJECTIVES OF THE WORK

The research targets to develop a self-sensing cementitious (SSC) composites using industrial-based nanofillers such as Graphene oxide (GO) & Reduced graphene oxide (rGO) for smart structural health monitoring. Main objectives of the proposed research work can be obtained as:

- Evaluating the impact of various GO doses and design mixtures on the mechanical characteristics of Portland cement-based mortars cured over short- and long durations.
- Evaluating the impact of various rGO doses and design mixtures on the mechanical characteristics of Portland cement-based mortars cured over short- and long durations.
- Monitoring the electrical properties such as piezo-resistivity of GO based developed sensors on cement mortar specimens under monotonic compressive loading.
- Monitoring the electrical properties such as piezo-resistivity of rGO based developed sensors on cement mortar specimens under monotonic compressive loading.

1.6 ORGANISATION OF THESIS

The thesis report consists of 5 chapters.

Chapter 1 – Provides an introduction to SSC composites, different types of nanomaterials and their properties.

Chapter 2 – Deals with the study of various researchers on various nanofillers such as GO, rGO, CNTs, GNPs, GP and other graphene-based nano-fibres, their effect on different self-sensing properties such as electrical resistivity and piezo-resistivity and mechanical properties.

Chapter 3 – Details the scheme of experimentation, materials used and variables involved. Information about mortar mix design is also illustrated in this chapter.

Chapter 4 – Presents the results and their analysis for mechanical properties such as compressive strength and flexural strength. This chapter also presents the results and analysis of electrical properties such as electrical resistivity and piezo resistivity.

Chapter 5 – summarizes and concludes the findings of the study and the future scope is discussed.

References are placed at the end.

CHAPTER 2
REVIEW OF LITERATURE

2.1 GENERAL

This chapter deals with the literature work done by various authors across the years on the properties of Graphene oxide (GO), Reduced Graphene oxide (rGO), Carbon nanotubes (CNTs), Graphene nanoplates (GNP), Pristine graphene (PRG) and other graphene derivatives when added to cementitious composites. Studies properties were grouped into two main categories which are mechanical properties and self-sensing properties. Mechanical properties include compressive and flexural strength, whereas, self-sensing properties involve the study of the main sensing mechanism through testing such as piezo-resistivity and electrical resistivity.

A wide range of mechanical, electrical, and thermal characteristics may be obtained and successfully integrated into nanomaterials because of the relatively adjustable characteristics of GO and rGO. GO and rGO have a broad array of applicability and hold promise as a key component in the development of innovative and better goods. Thus, GO and rGO were selected for inducing self-sensing behaviour in the cementitious composite.

GO material does, however, have several drawbacks that could affect how well it performs in cementitious composites. It possesses mechanical characteristics that are significantly less than those of PRG or rGO because it is less crystalline, has a large degree of imperfections. Consequently, the overall structural properties of cement-based composites are projected to be improved with the application of PRG and rGO in cementitious composites.

Despite having greater mechanical qualities in comparison to GO, graphene nanomaterials like rGO and PRG are extremely hydrophobic and less water-dispersible, this is why it is less desirable to include them into cement composites to improve cement performances.

2.2 EFFECT ON MECHANICAL PROPERTIES OF CEMENTITIOUS COMPOSITES

GO is a water-compatible, highly dispersible oxygenated derivative of graphene produced by acid oxidation of graphite. This is one of the factors that led to the selective exploration of GO as an addition for enhancing cementitious composites' mechanical capabilities. Since GO is extremely dispersive in water and possesses an excess of oxygen-functional groups, there has

been considerable interest in employing GO to enhance the characteristics of cementitious composites in the literature (ref).

Lv et al., (2013) researched on the impact of GO on the microstructure and mechanical behaviour of cement composites. The experimental study demonstrated that incorporation of 0.03 percent GO to cement mortars may control the microstructures of the mortars as well as increase 28-day compressive strength, tensile strength, and flexural strength by 38.9 percent, 78.6 percent, and 60.7 percent, respectively.

According to **Lv et al., (2014),** 0.06 percent GO could increase the cement paste's compressive strength by 58.5 percent after 28 days, whereas 0.04 percent GO content could increase the cement paste's flexural strength by 67.1 percent after 28 days.

Wang et al., (2015) determined that after 28 days, compressive and flexural strength has shown an increase of 40.4 percent and 90.5 percent, respectively with 0.05 percent strength GO added to cement pastes.

Sharma and Kothiyal., (2015) also investigated the impact of various GO doses and sizes on the microstructures of cement mortars. The study demonstrated that the doses and sizes of GO had a significant impact on the characteristics of cement mortars. At a 1 percent GO content, the mixture with a smaller GO dimension (i.e., 100nm) increases compressive strength by 86 percent. This increase is greater than the 63 percent improvement seen when employing the higher GO dimension (i.e.,900nm) at the same concentration. The significant impact of the oxygen-functional units of GO on the cement matrix is linked to the reinforcing action of GO on the mechanical characteristics of cementitious composites.

Mohammed et al., (2016) demonstrated that a cement mortar mix with a 0.03 percent GO addition may boost compressive strength by 30 percent after 28 days.

The reinforcing process of the structural strengths of GO cement-based composites is controlled by chemical interactions between hydroxyl and carboxyl groups of GO and the mediating Ca^{2+} ions from calcium silicate hydrate of cementitious gels, as per the study by **Hou et al., (2017**) and **Pan et al., (2015).** (**Figure 2.1**). In the cement-based matrix, this creates a space framework that increases the cementitious composite materials' ability for load transfer.

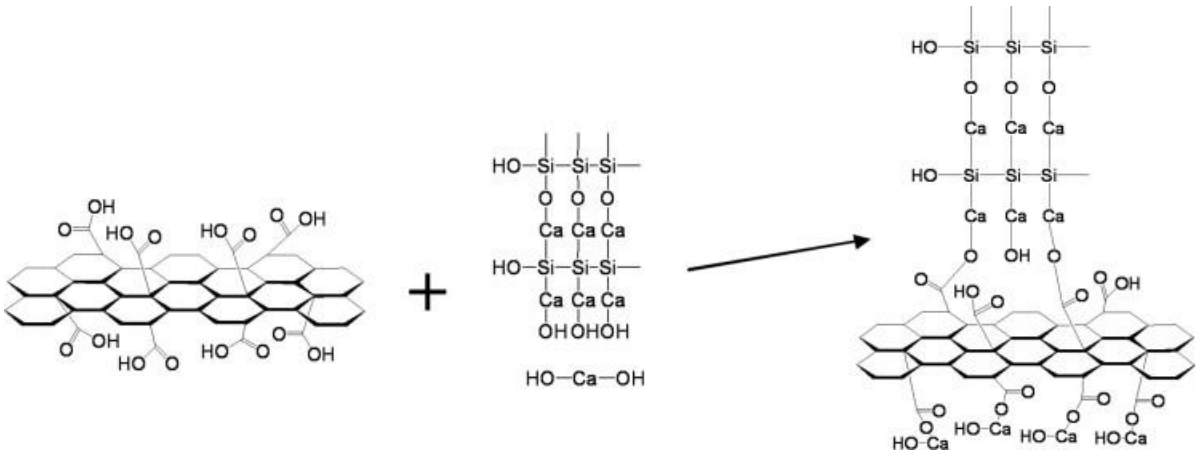

Figure 2.1 Representation of the interaction between GO and hydration molecules, (Pan et al, 2015)

Dong et al., (2021), studied the effects of Graphene Nanoplate (GNP) and Graphite Plate (GP) and the piezo-resistive characteristics of cement mortar specimens were examined along with the physiochemical and mechanical properties. This study examined four distinct GNP and GP dosages of 0.5 percent, 1.0 percent, 2.0 percent, and 3.0 percent by weight of binder (total of cement and silica fume). The related composites were denoted as GNPC05, GNPC1, GNPC2, and GNPC3, respectively.

They found that compressive and flexural strengths for the GNP-filled specimens increased initially, then dropped as the GNP concentration increased (**Figure 2.2**). Compressive and flexural strengths of the cementitious composites with the highest mechanical properties achieved were 53.6 MPa and 3.6 MPa, respectively, when GNP content was optimised to 1 percent. As the GNP dosage reached 2 percent, the strengths started to significantly decline.

It appeared that, in contrast to the GNP composites, the GP achieved very little progress in terms of the mechanical characteristics of cement specimens. In the case of a tiny dose of GP of 0.5 percent, the compressive and flexural strengths only marginally increased; however, as GP concentration grew, the strengths decreased drastically. The compressive and flexural strengths decrease rates for the GPC3 peaks at 18.9 percent and 17.2 percent, respectively (**Figure 2.3**).

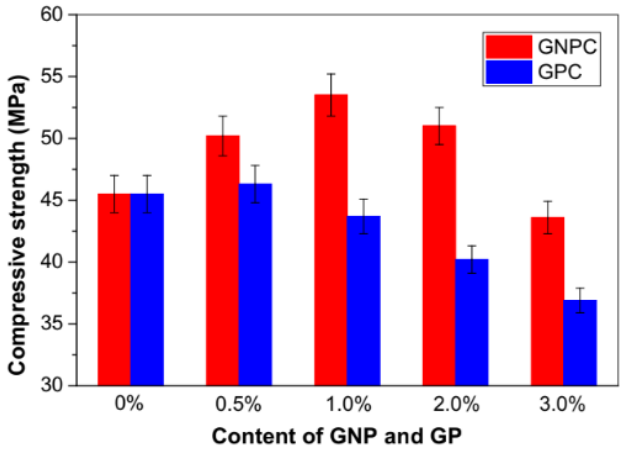

Figure 2.2 Results of Compressive Strength with varying % of GNP/GP, (Dong et al, 2021).

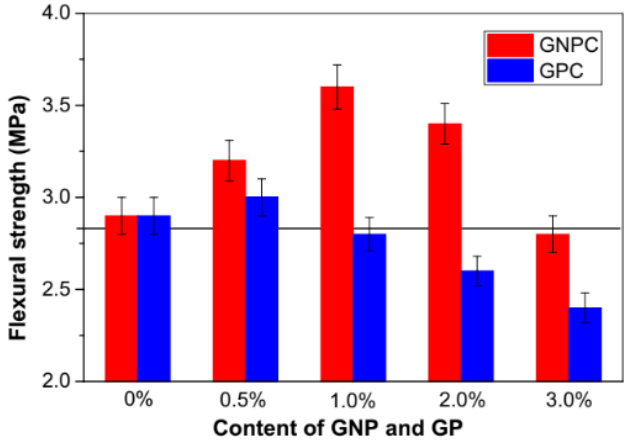

Figure 2.3 Results of Flexural Strength with varying % of GNP/GP, (Dong et al, 2021)

Only a few research studies have looked at how rGO affects the characteristics of cementitious composites. According to **Murugan et al., (2016)**, adding 0.02 percent rGO into a cement mixture might not only improve the mix's 28-day compressive and flexural strengths by roughly 22 and 23 percent, respectively, but also improve the mix's voids and capillary pores. **Qureshi and Panesar., (2019)** looked at how various rGO doses affected the characteristics of cementitious material. According to the research, 0.06 percent rGO might increase the cement paste's compressive and flexural strengths at 28 days by 14.9 and 33.7 percent, respectively.

In the work of **Kiamahalleh et al. (2020)** the effect of various rGO dimensions on the mechanical characteristics of cement-based mortars was successfully demonstrated. The findings revealed that the mix containing 0.1 percent rGO with the smallest dimension had 28-day compressive and tensile strengths that were, respectively, 91 and 52.5 percent greater than the plain.

Graphene comes in a variety of forms with various functionalities and physical characteristics, including graphene oxide (GO), reduced graphene oxide (rGO), pristine graphene (PRG), doped graphene, and functionalized graphene.

Parvez et al., (2014) found that when compared to rGO, the PRG produced through an electrochemical approach of direct exfoliation from graphite exhibits various characteristics, including fewer flaws, higher crystalline nature, and greater conductivity (**Figure 2.4**).

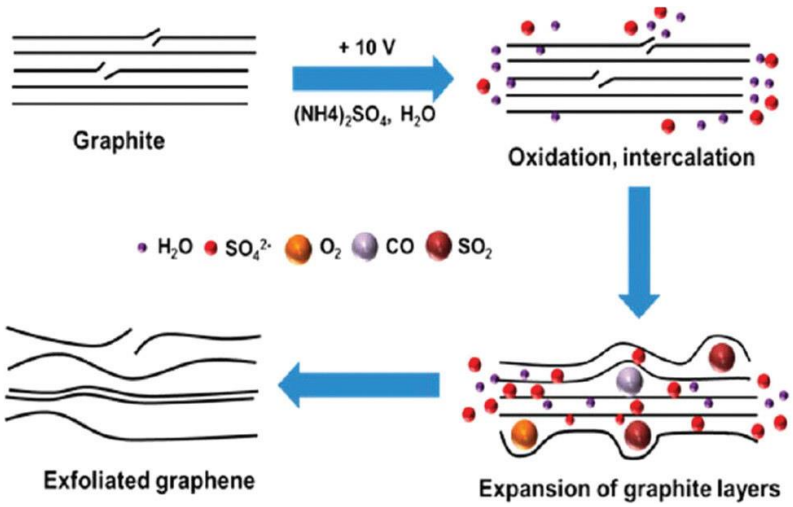

Figure 2.4 Graphene synthesis using electrochemistry, (Parvez et al, 2014)

Du and Pang., (2015) examined the properties of mortar mixes with 4 different PRG dosages (i.e., 0%, 2.5%, 5.0%, and 7.5%) and PRG size (8 m), and demonstrated how the inclusion of PRG may significantly decrease the degree of water penetration. Their investigation confirms that PRG has no impact on the mortar's compressive and flexural strengths. Due to the increased PRG dosages employed, PRG sheets aggregated and formed multi-layered PRG films, which prevented PRG from interacting with the cement matrix. As per a recent investigation of PRG-cement mortars with various PRG doses (i.e., 0 percent, 0.05 percent, 0.1 percent, 0.5 percent, and 1 percent by weight of cement, with PRG size 5-10 m), 0.05 percent PRG additive can increase compressive strength and flexural strength at 28 days by nearly 8.3 percent and 15.6 percent, respectively. Due to the agglomeration of PRG, the strengths begin to decrease when the PRG dose is increased to more than 0.05 percent.

Tao et al., (2019) did research on the cyclic compressive loading on cement mortar. Investigations were done into how (GNPs) affected the mechanical, and electrical characteristics of cementitious mortar mix.

The preparation of mortars with GNPs ranging from 0% to 1% was accomplished. In total, 5 different specimens were prepared for the testing namely M0, M1, M2, M3 and M4. They reported that both the compressive strength as well as the flexural strength typically rise initially before declining as the GNP content rises (**Figure 2.5**). The highest results were discovered for M1 sample which only featured 0.05 percent GNPs with respect to cement. The values of M1 are increased from 49.5 MPa and 7.7 MPa to 53.6 MPa (by 8.3 percent) and 8.9 MPa (by 15.6 percent), respectively, in comparison to the compressive and flexural strengths of M0.

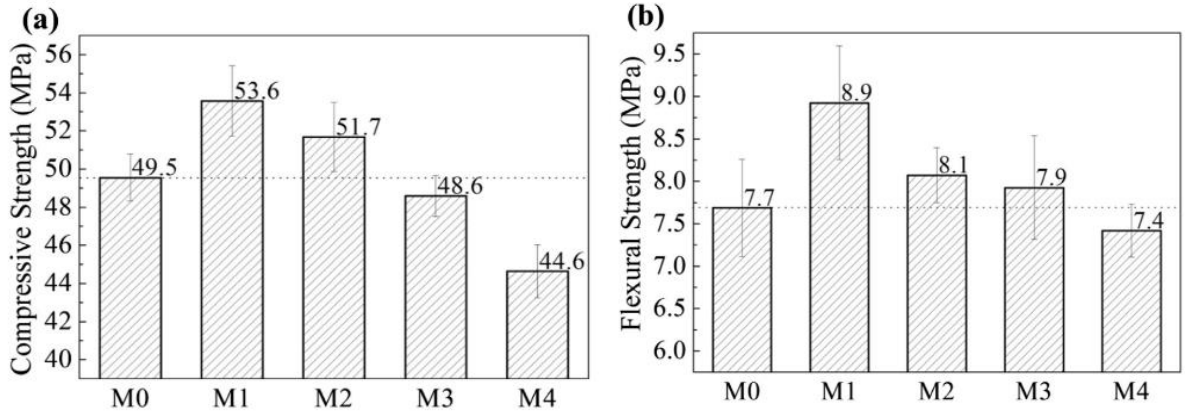

Figure 2.5 Results of (a) Compressive Strength and (b) Flexural Strength, (Tao et al, 2019)

They concluded that compressive and flexural strengths decline monotonically and consistently as the GNP concentration rises over 0.05 percent. However, when the concentration of GNPs doesn't quite exceed 0.5 percent, the mechanical characteristics can be enhanced and/or maintained.

Based on the literature of various authors on mechanical properties it was found that graphene based nanofillers are very useful for enhancing the mechanical properties for cement-based composites. But it was also reported that on increasing the dosage of nanofillers such as GO, rGO, CNTs, PRGs from optimum content, there was a sharp decrease in the mechanical properties.

2.3 EFFECT ON ELECTRICAL AND SELF-SENSING PROPERTIES OF CEMENTITIOUS COMPOSITES

Cement-based composites with only 0.38% CF and a hybrid with 0.18% CF and 15% carbon black particles were both studied by **Ou et al., (2008)** for their electrical performance (**Figure 2.6**). Until the sensors failed, the sensors were subjected to a linearly increasing compressive

stress. It was demonstrated that the hybrid had superior linearity and repeatability when measuring the FCR. The improvement of the contacting and tunnelling conduction action was shown to be the cause of this phenomenon.

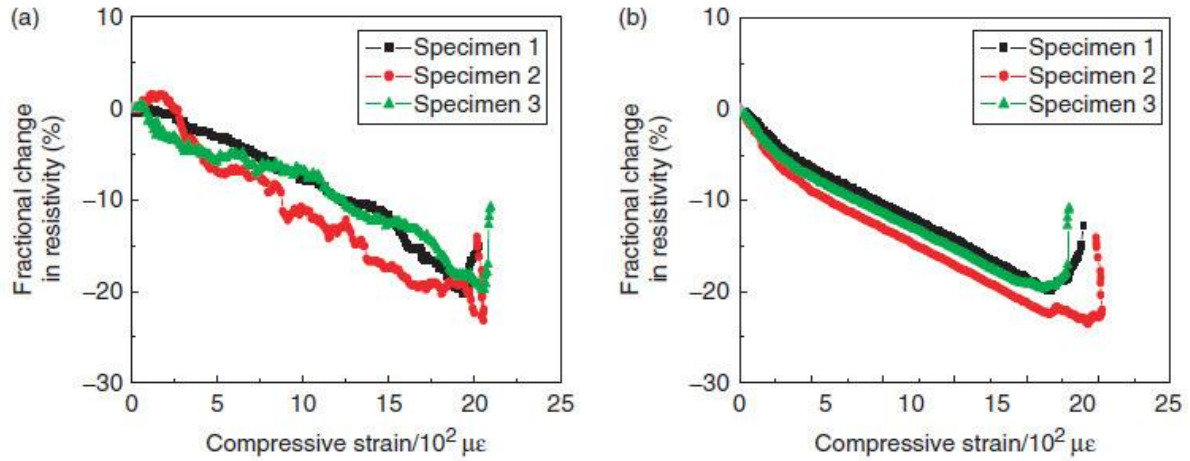

Figure 2.6 Comparison of Fractional change in resistance under compressive strain, (Ou et al, 2008)

Azhari et al., (2012) measured resistivity using cement-based sensors that had various CF volume percentages. Although the resistivity was greatly reduced, the composite seemed much more brittle once the CF concentration reached 20%. The amount of CF was reduced to prevent the structure from becoming brittle. A 1% vol. increase naturally lowered the resistance because of the material's high surface area and outstanding electrical properties. FCR may be used to describe the general sensing response of cement-based sensors under compression. The resistivity of the specimen drops as the compressive stress rises, producing a negative FCR. If stresses did not surpass the composite's elastic range, the FCR rises to its starting value upon sensor unloading, **Azhari & Banthia., (2012).**

Saafi et al., (2014) investigated the self sensing capabilities of fly assh based geopolymeric composites incorporating with varying content of rGO as 0 percent, 0.1 percent and 0.35 percent. The electrical propteries such as conductivity & piezo-resistivity were evaluated under tension and compression. They found that the rGO increased the electrical conductivity of the fly ash-based rGO geopolymeric composites from 0.77 S m^{-1} at 0.0 wt% to 2.38 S m^{-1} at 0.35 wt%. the electrical conductivity of the geopolymeric composites increases as the rGO content

increases. The experimental results showed electrical conductivity gains of 96% and 209% upon adding 0.1 and 0.35 wt% rGO, respectively (**Figure 2.7**). These gains are due to the formation of uniformly distributed rGO conductive networks within the composites. The rGO also increased the gauge factor by as much as 112% and 103% for samples subjected to tension and compression, respectively.

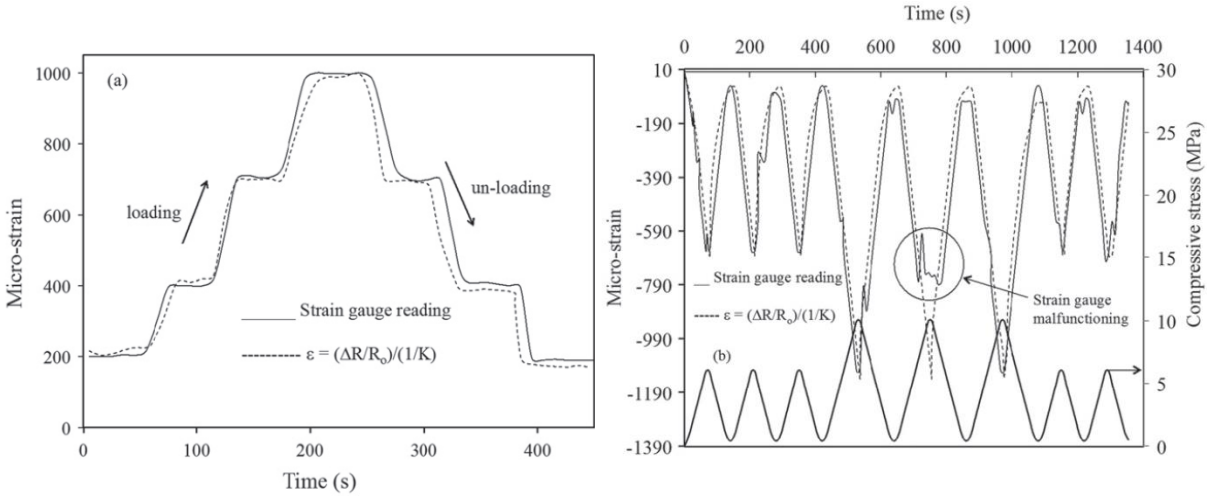

Figure 2.7 Respnse of rGO composites under (a) Tension (b) Compression. (Saafi et al, 2014)

The electrical behaviour of CNTs and carbon nanofibers (CNF) in cement paste was studied by **Konsta-Gdoutos et al., (2014).** CNTs and CNFs were added to the cement composites in amounts of 0.048, 0.1, and 0.3 wt% (volume percent of cement). The resistivity properties of unloaded sensors were first assessed. A certain voltage amplitude was confirmed in order to get reliable and consistent results. The ideal amplitude for measurements of the electrical resistance seemed to be 20 V of voltage. The results revealed that CNTs, particularly at greater volume fractions, produce a lower cement composite resistivity than CNF (**Figure 2.8**).

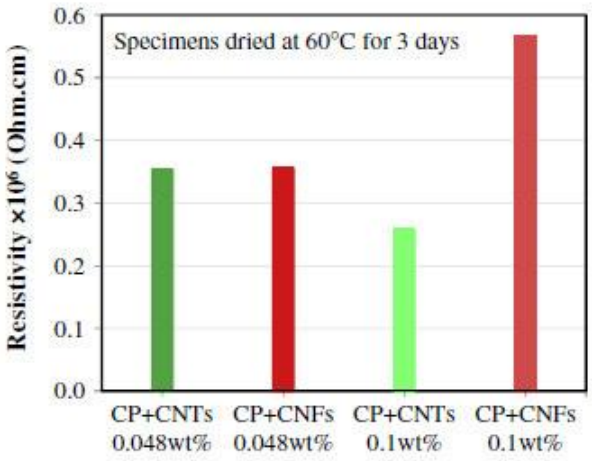

Figure 2.8 CNT and CNF-based composites with an average resistivity comparison, (Konsta-Gdoutos et al, 2014).

The amount of useful filler particles in the cementitious mixture affects how electrical resistivity changes. **Figure 2.9** shows how they are related to one another. The percolation phenomena can be seen in the curve, and its presence is explained by varied functional filler concentrations, **Han et al., (2014)**. The curve may be split into three zones: zone A, which has a higher resistivity value, zone B, which has a sharp decline in resistivity, and zone C, 2which has a lower resistivity value (**Figure 2.9**).

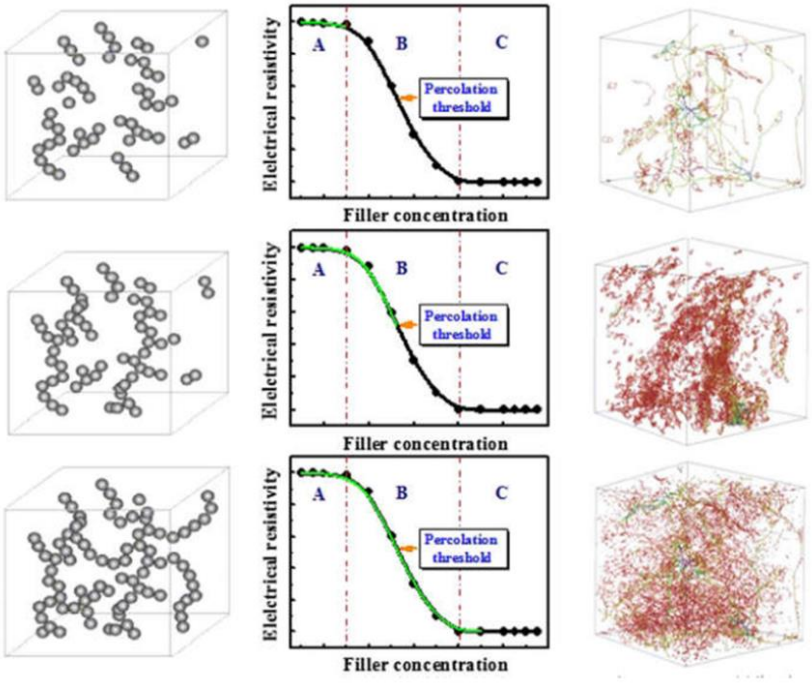

Figure 2.9 Variation of the electrical resistivity with change in filler concentration, (Han et al, 2014).

It has been stated in several articles that the electrical properties of rGO and CNTs are exceptional. rGO & CNTs may be used to create materials with piezo-resistive self-sensing capabilities that have an electrical behaviour that is virtually insulating. CNTs significantly boost the electrical conductivity of cement-based composites while lowering their electrical resistance to almost 1Ωcm. Electrical properties are very reliant on the amount and dispersion of CNTs, similar to mechanical properties. Agglomerates of CNTs will result in abnormalities in the conducting network, reducing the composite's piezo-resistivity **(Sun et al., 2015).**

The CNT concentration of a cement-based composite for strain sensing should be close to the percolation threshold in order to obtain lower resistance and strong sensitivity. A shift in intrinsic resistance occurs when a piezoresistive cement-based composite is deformed. This indicates that each CNT's resistance varies as well, although because with its tiny size and high

Young's modulus, this effect is comparatively insignificant in terms of the piezoresistive sensing of the entire composite.

The difference in contact resistance between the CNTs is another element that affects how well an electrical current flow through a cement-based composite. The tension and compression will cause the fibres to shift closer or further apart, which will significantly alter the sensing behaviour. The sensitivity increases with the fibre content's proximity to the percolation threshold and the quality of the fibre dispersion. Changes in contact resistance and tunnelling distance are closely related. According to this process, the behaviour of electrons hopping across CNTs varies with their proximity (**Figure 2.10**).

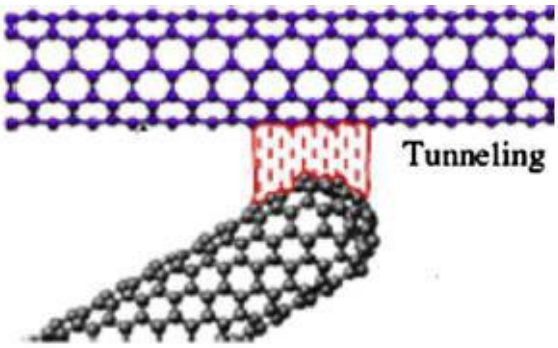

Figure 2.10 The tunnelling phenomenon between neighbouring CNTs, (Sun et al., 2015).

A small fibre push-in that occurs when a crack closes helps elucidate why resistivity decreases under compressive loads. Additionally, as conductive particles get closer together, their tunnelling distance and contact resistance get reduced as well. Conversely, the slight fibre pull-out that occurs when a fracture open is followed by a rise in resistivity under tension (**Figure 2.11**). As tunnelling distance grows, contact resistivity must also rise **(Chung, 2016).** In order to quantify the length of a propagating crack, the researchers **Reza et al., (2004)** discovered that electrical resistance may be employed to examine the mechanics of the fracture process zone in an investigation of concrete with CF under compact tension's self-sensing behaviour.

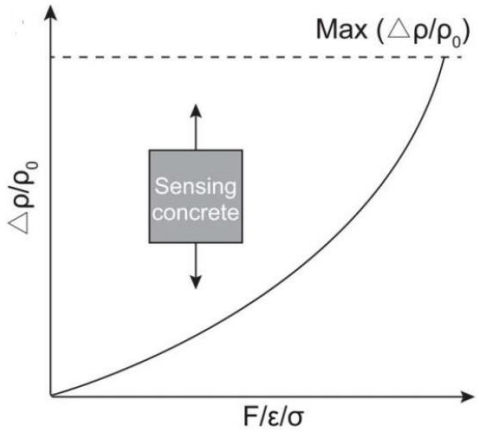

Figure 2.11 Self-sensing concrete under monotonic tension. (Ding et al, 2019).

Yoo et al., (2019) investigated the impact of different carbon nanomaterial types and quantity on the electrical characteristics of cement paste. The self-sensing capability of cementitious composites containing five different carbon nanomaterials, including carbon nanotubes (CNT), carbon fibres (CF), graphite nanofibers (GNF), graphene (G), and graphene oxide (GO), was investigated. It was discovered that adding the nanomaterials decreased the electrical resistivity of plain cement paste. While adding CNT improved the conductivity of cement composites most effectively at high volume fraction, using CF was most successful at boosting it at low volume fraction (**Figure 2.12**).

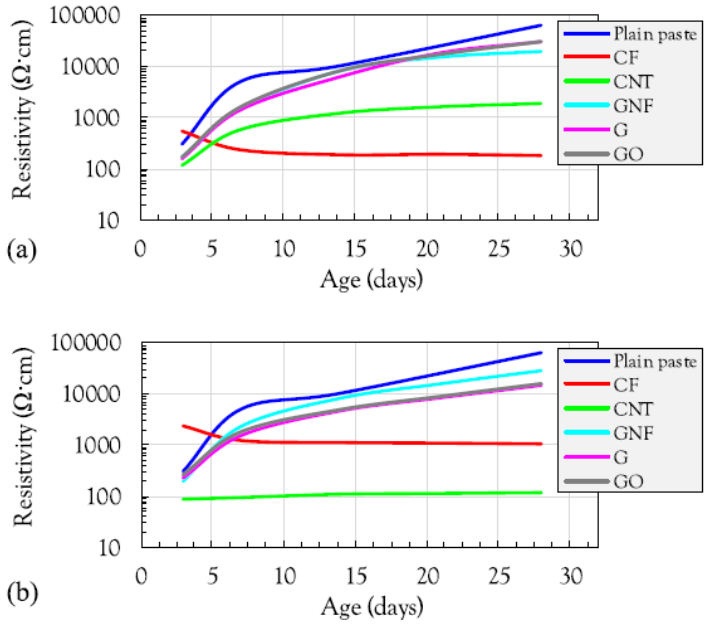

Figure 2.12 Electrical resistivity of cement composites; (a) vf of 0.5%, (b) vf of 1.0%, (Yoo et al, 2019)

Tao et al, (2019) researched on the cyclic compressive loading on cement mortar. Investigations were done into how (GNPs) affected the mechanical, and electrical characteristics of cementitious mortar mix. The preparation of mortars with GNPs ranging from 0% to 1% was accomplished. In a total, 5 different specimens were prepared for the testing namely M0, M1, M2, M3 and M4.

They discovered that raising the GNP concentration can reduce the cement mortars' electric resistivity under free loads (**Figure 2.13**). A percolation rule governs the connection between the electric conductivity and the content percentage of GNPs.

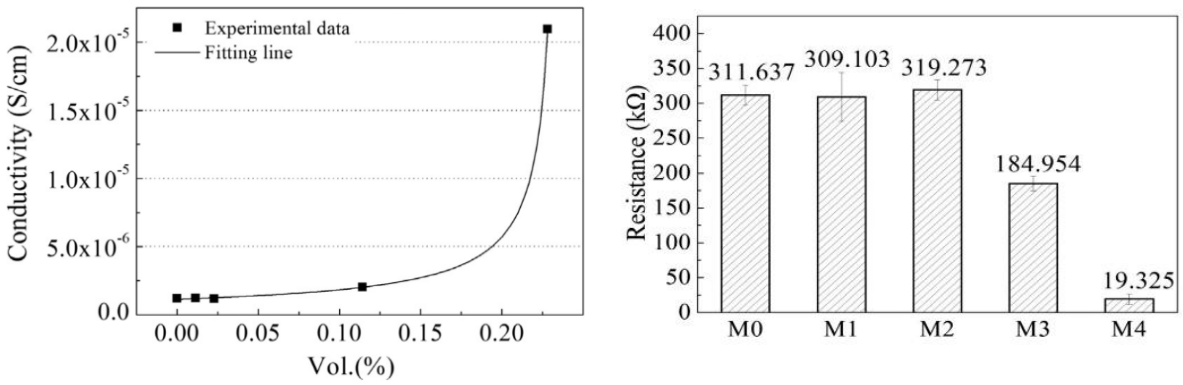

Figure 2.13 Variation of conductivity and electrical resistivity**, (**Tao et al, 2019)

They also reported that the filling and interfacial influences control the piezoresistive behaviour of the GNP modified cementitious mix (**Figure 2.14**). The considerable deterioration of gauge factors with loads is caused by the GNPs and mortar matrix's poor interfacial connections. The interfacial impact diminishes for the mortar specimens with strongly linked GNPs

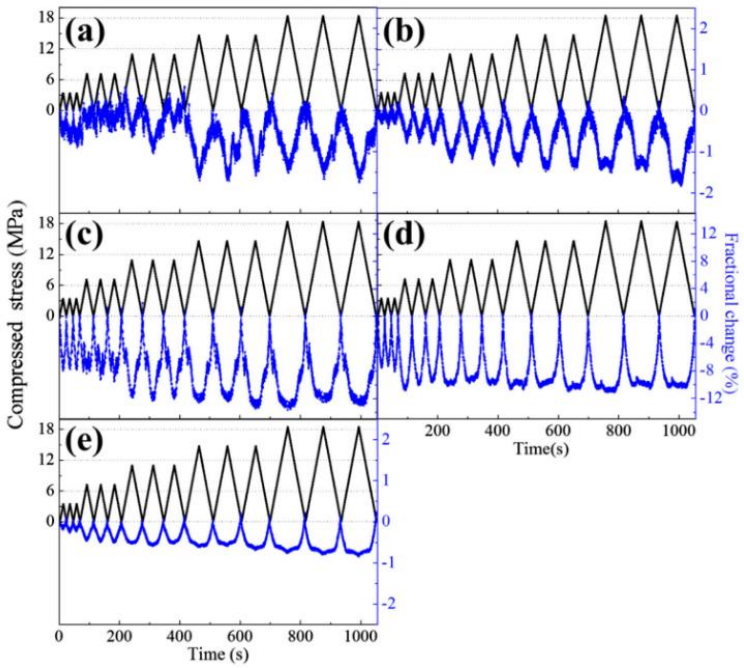

Figure 2.14 Time history relationship b/w FCR and Stress for (a) M0, (b) M1, (c) M2, (d) M3 and (e) M4, (Tao et al, 2019)

Wang and Zhang (2022) investigated FCR and cyclic compressive stress/strain of specimens during 28 days of curing period under 20 MPa of stress are correlated throughout time. M6 and M0 have respective maximum stresses of 66.0 MPa and 96.5 MPa. M6 means content of GNPs/CNTs is 6 wt%. Whereas, M0 means content of GNPs/CNTs is 0 wt%. Both M6 and M0 can experience deformation when operating in an elastic domain, and their distortion can be recovered when subjected to cyclic compression. According to **Figure 2.15**, M6's FCR

decreases with rising compressive stress/strain and vice versa. 9.86 percent is the FCR's absolute maximum bound. There is high repeatability and stability in the time history connections between FCR and the cyclic compressive stress/strain of M6.

As shown by the **Figure 2.16**, connections between FCR and cyclic stress/strain of M0 are comparable to those of M6. However, compared to M6, the absolute maximum FCR of M0 is significantly lower at 0.53 percent. Moreover, polarization-related interactions between FCR and cyclic stress/strain of M0 show a minor increasing tendency.

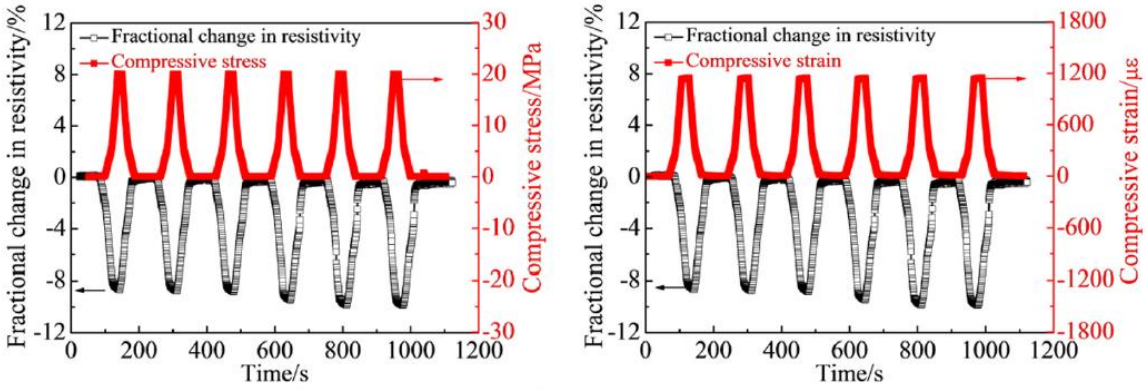

(a) Time history relationship between FCR and cyclic compressive stress

(b) Time history relationship between FCR and cyclic compressive strain

Figure 2.15 (a) Time history relationship between FCR and cyclic compressive stress (M6), (b) Time history relationship between FCR and cyclic compressive strain (M6).

(Y. Wang and L. Zhang, 2022)

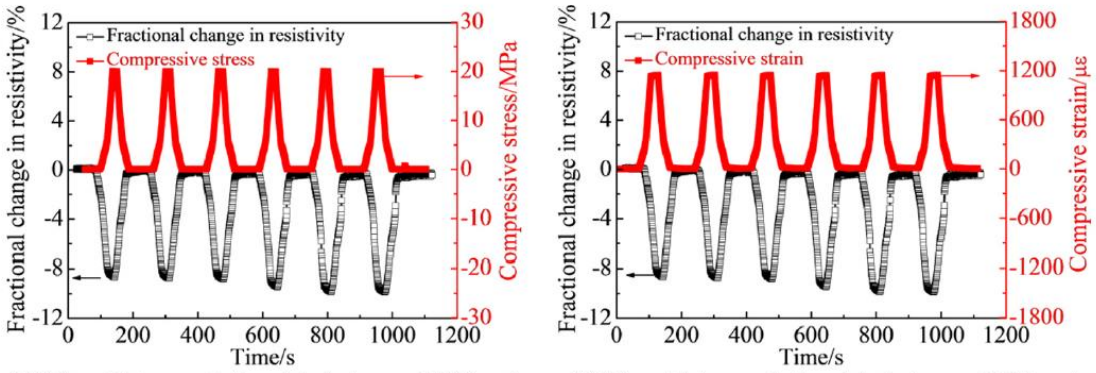

(a) Time history relationship between FCR and cyclic compressive stress

(b) Time history relationship between FCR and cyclic compressive strain

Figure 2.16 (a) Time history relationship between FCR and cyclic compressive stress (M0), (b) Time history relationship between FCR and cyclic compressive strain (M0).

(Y. Wang and L. Zhang, 2022)

The stress sensing capabilities of cement-based sensors with and without various surface alterations was studied by **Dong et al., (2022).** After applying surface coatings, the impact of coatings on piezo resistive sensitivity was examined. Compared to commercially existing strain gauges, the sensitivity of cement-based sensors was hundreds of times higher. In the loading and unloading procedures, resistivity initially reduced and then restored, showing that all cement-based sensor's FCR had a good connection to the compressive stress (**Figure 2.17**). The highest FCR value was 12.6 percent for the graphene-filled cement-based sensor that wasn't coated. This was followed by average FCRs of 7.7 percent, 7.2 percent, and 5.3 percent for cement-based sensors that had been coated once, twice, or without isopropanol, respectively.

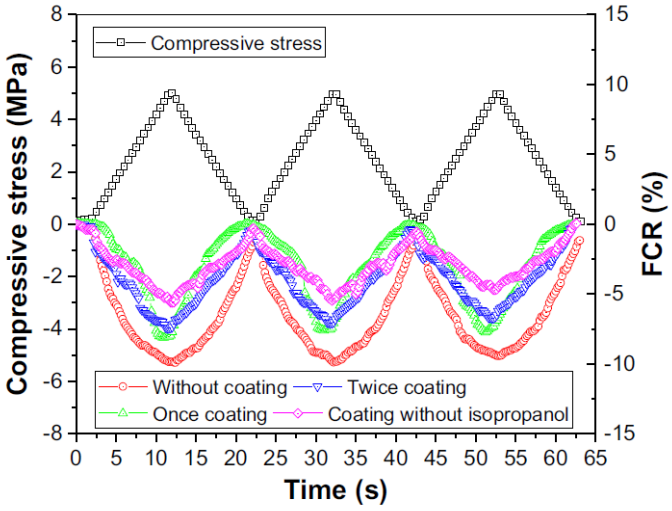

(a) Stress sensing

Figure 2.17 Self-sensing capacities of cement-based sensors with different surface modification treatments, (Dong et al, 2022).

2.4 SUMMARY

Researches are still far away from the prediction of sensing properties of GO & rGO cement-based specimens, according to the examination of numerous literatures on the electrical properties such as piezo-resistivity, electrical resistivity, and stress sensitivity. Experimental self-sensing tests have been carried out in this thesis for varying percentages of GO and rGO cement-based specimens.

2.5 RESEARCH GAPS

1) Limited research on the use of Graphene Oxide (GO) and reduced Graphene Oxide (rGO) for inducing self-sensing behaviour in concrete.

2) Research on piezoresistive capacities of cement comprising GO/rGO is still rare, despite the publication of a few studies on electrical properties.
3) Effect of the external environment such as temperature, carbon dioxide, chloride content, and humidity on the sensing performance of SSC is yet to be explored.
4) Application of SSC for other areas such as corrosion monitoring and crack detection are other potential applications in the construction industry that need to be discovered.

CHAPTER 3
EXPERIMENTAL DESIGN AND METHODOLOGY

3.1 GENERAL

The main objective of the experimental research is to investigate the properties of cement mortar on addition of different percentages of Graphene Oxide (GO) & Reduced Graphene Oxide (rGO). GO and rGO were incorporated as filler in varied proportions to cement mortar specimens with a cement to sand ratio of 1:3. The Water/Cement ratio was maintained at 0.35. The mechanical and microstructural properties of the specimens were examined. The fundamental evaluations on cement mortars are covered in this chapter.

3.2 MATERIALS USED

3.2.1 Ordinary Portland Cement Grade 43 (OPC- 43)

Ordinary Portland Cement of Grade 43 (OPC-43), which complied with the code IS:8112-1989 of BIS (Reaffirmed 2005) has been utilized in each of the experiment. The cement was from same batch. The characteristics of OPC- 43 as per manufacturer are shown in the Table 3.1 below:

Table 3.1 Physical characteristics of OPC-43 used.

PHYSICAL CHARACTERISTICS	VALUES AS PER IS:8112-1989
Initial Setting time (minutes)	Not less than 30
Final setting time (minutes)	Not less than 600
Fineness (%)	10 max.
Specific Gravity	3.15 max.
Compressive Strength	
3 Days (N/mm^2)	23
7 Days (N/mm^2)	33
28 Days (N/mm^2)	43

3.2.2 Standard Sand

Indian Standard sand of 3 grades (Grade 1, Grade 2 & Grade 3) was used throughout the research. Standard sand was procured from Ambala, Haryana. The specifications provided by

the vendor are listed in **Table 3.2**, and they correspond to the IS:650-1991 regulations for specifications.

Table 3.2 Particle size specifications of Standard Sand

GRADE	PARTICLE SIZE SPECIFICATION OF STANDARD SAND (MM)	% USED AS PER CASTING.
I	1-2	25
II	0.5-1	50
III	0.09-0.5	25

3.2.3 Water

Since charged particles from the natural surroundings, pipelines, and other sources exist in ordinary tap water. Usually, with the use of nanofillers, deionized water is utilized for scientific and research applications. Deionized water was used for all the experimental mixing except the curing process in which normal tap water was used.

3.2.4 Superplasticizer

Auramix-400 was used as a superplasticizer in the mix. It is a high-performance superplasticizer developed on Poly-carboxylic Ether (PCE) based technology that's designed for applications that demand a significant impact on water reduction and workability retention. As per the manufacturer, Auramix-400 attributes are shown in **Table 3.3** below:

Table 3.3 Characteristics of Auramix-400

PROPERTIES	
Appearance	Light yellow coloured liquid
pH @27°C	Minimum 6.0 Maximum 8.0
Volumetric mass @ 20°C	1.09 kg/litre
Chloride content	Nil to IS:456
Specific gravity	1.205-1.215
Alkali content	Typically, less than 1.5g Na_2O equivalent/litre of admixture.

3.2.5 Stainless Steel Plates

Stainless steel (Grade 304) plates were used for testing electrical properties. These plates were installed in the samples during the casting process in electrical and piezoresistive specimens (**Figure 3.5**). The specifications of the plates used can be seen in **Table 3.4**:

Table 3.4 Specification details of Stainless-steel plates

GRADE OF STAINLESS-STEEL	TYPE OF MORTAR MIX	SPECIFIED SIZE OF PLATE IN (MM)	NO OF PLATES FOR EACH SPECIMEN	SPACING BETWEEN PLATES (MM)
304	Cube	20×75×1	4	10
304	Prism(beam)	40×60×1	4	• 60 (between internal plates). • 30 (between external plates).

3.2.6 Graphene Oxide

Graphene oxide (GO) is a one-of-a-kind substance that consists of a single monomolecular layer of graphite with epoxide, carbonyl, carboxyl, and hydroxyl groups (Koh et al, 2014). (**Figure 3.1**).

Figure 3.1 GO used.

Table 3.5 Specification details for GO used.

GRAPHENE OXIDE	DESCRIPTION
Purity	~99%
Thickness (Z)	~0.8-2nm
Average lateral dimension (X & Y)	~5-10µm
Number of layers	1-3 Layers
Carbon content	~60-80%
Oxygen content	~15-32%
Hydrogen content	~1-2%
Nitrogen content	~1-2%
Sulfur content	<1%
Surface area	110-250* m^2/g
Bulk density	$0.5g/cm^3$
Chemical formula	C
Physical form	Fluffy, very light powder

The XRD pattern of GO revealed peak at 2θ of 11.7° with d-spacing of 0.76nm, depicting successful oxidation of graphene to GO **(Figure 3.2)** This is mainly due to presence of oxygen-containing functional groups attached on both sides of the graphene sheet. The large interlayer spacing (d-spacing) observed in GO is due to presence of hydroxyl, epoxy, and carboxyl groups (Gurunathan et al. 2012). SEM image **(Figure 3.3)** of GO showed smooth sheets with small wrinkles and folded at the edges (Huang et al. 2018)

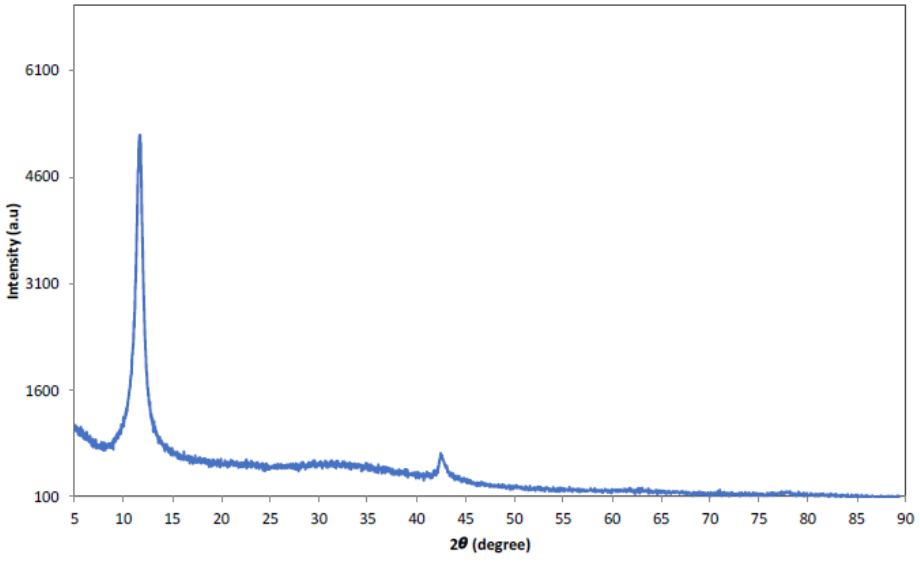

Figure 3.2 XRD of Graphene Oxide.

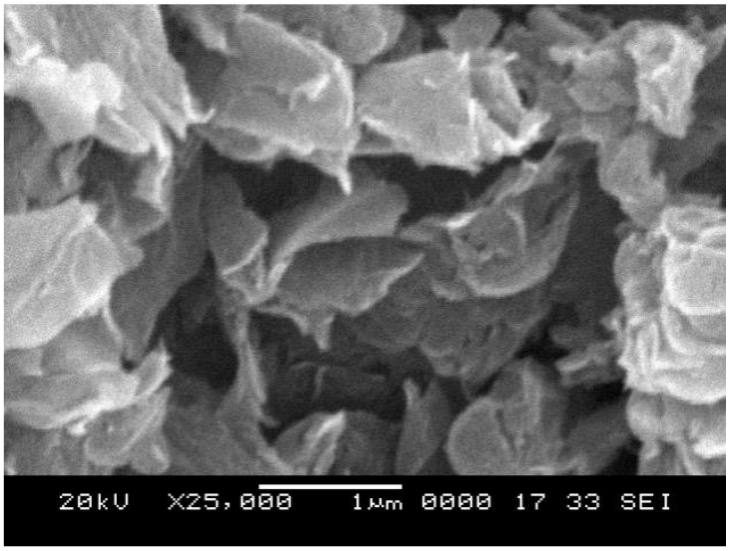

Figure 3.3 SEM image of Graphene Oxide.

3.2.7 Reduced Graphene Oxide

Reduced graphene oxide (rGO) is a form of graphene oxide that has undergone chemical, thermal, and other processing to reduce the oxygen amount (Qureshi 2020). It is a fluffy, very-light black powdered nanofiller (**Figure 3.4**). The oxygen content present in rGO ranges from 5-10% as compared to GO which has 15-32% oxygen content respectively.

Figure 3.4 rGO used.

Table 3.6 Specification details for rGO used.

REDUCED GRAPHENE OXIDE	DESCRIPTION
Purity	~99%
Thickness (Z)	~0.8-2nm
Average lateral dimension (X & Y)	~5-10µm
Number of layers	1-3 Layers
Carbon content	~85-92%
Oxygen content	~5-10%
Hydrogen content	~1-2%
Nitrogen content	~1-2%
Sulfur content	<1%
Surface area	80-200* m^2/g
Bulk density	$0.03g/cm^3$
Chemical formula	C
Physical form	Fluffy, very light powder

rGO is formed after reduction of GO, which leads to disappearance of 2θ peak at 11.7°. Instead, a peak was observed at 26° with d-spacing of 0.34nm **(Figure 3.5)**. The reduction of GO leads to tighter packing of rGO, thus resulting in decrease in interlayer spacing, which is mainly attributed to removal of some oxygen-containing functional groups (Gurunathan et al. 2012). The rGO SEM picture **(Figure 3.6)** revealed that the substance is made up of tiny, crumpled sheets that are layered and aggregated and intimately connected to one another to form a disordered solid (Huang et al. 2018).

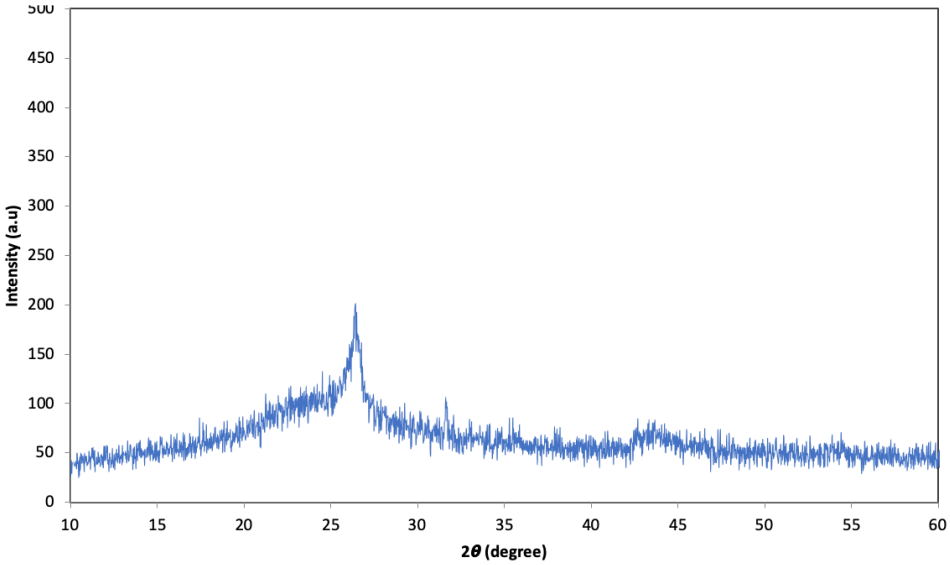

Figure 3.5 XRD of Reduced Graphene Oxide

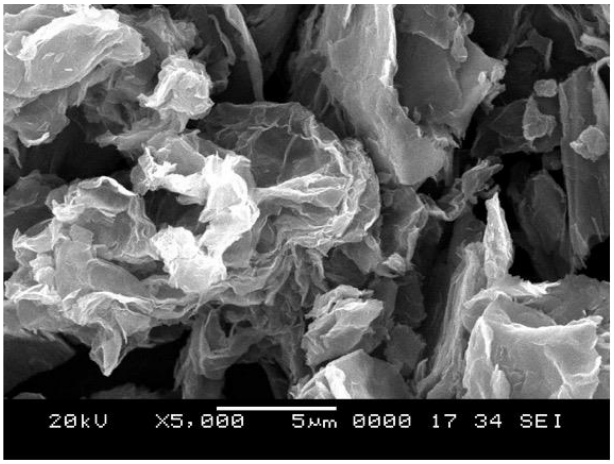

Figure 3.6 SEM image of Reduced Graphene Oxide.

3.3 Batching, Mixing and Casting of Specimens

3.3.1 Cement Mortar Samples with GO and rGO.

Mortar samples were made following ASTM specifications, using a cement-to-sand ratio of 1:3. GO and rGO were first ultrasonically mixed in deionized water before being integrated into the mortar matrix.

A set of three different GO cement-based mortar cube specimens were made referred to as GO-M1, GO-M2 and GO-M3 respectively. (**Table 3.7**)

Three other mixes of rGO cement-based cube specimens with different doses of 0.06, 0.08, and 0.1 percent by weight of cement were prepared and are designated as rGO-M1, rGO-M2 and rGO-M3 respectively.

Table 3.7 Mix proportions of cementitious cube specimens with GO & rGO.

MIX	Cement (kg/m^3)	Grade I Sand (kg/m^3)	Grade II Sand (kg/m^3)	Grade III Sand (kg/m^3)	Water (kg/m^3)	Superplasticizer (%)	GO (kg/m^3)	rGO (kg/m^3)
Control	568.32	426.24	852.48	426.24	198.4	0.8	-	-
GO-M1	568.32	426.24	852.48	426.24	198.4	0.8	0.57	-
GO-M2	568.32	426.24	852.48	426.24	198.4	0.8	1.14	-
GO-M3	568.32	426.24	852.48	426.24	198.4	0.8	1.71	-
rGO-M1	568.32	426.24	852.48	426.24	198.4	0.8	-	0.34
rGO-M2	568.32	426.24	852.48	426.24	198.4	0.8	-	0.45
rGO-M3	568.32	426.24	852.48	426.24	198.4	0.8	-	0.57

3.3.2 Dispersion of GO/rGO

The dispersion of Go/rGO fibres is a critical step in the creation of a cement-based self-sensing nanocomposite before using GO/rGO in dispersed form for casting. To establish a conductive network and lower the non-conducting matrix's resistivity, the GO/rGO must be dispersed uniformly throughout the cement matrix. Over the last few years, several ways for appropriately dispersing nanomaterials in cement matrix have evolved. Physical and chemical procedures are the two types of approaches available. Sonication, ball grinding, and mechanical stirring are examples of physical procedures, while chemical methods incorporate the use of dispersing agents to scatter nanomaterials.

Sonication rips apart clusters by supplying power to escape Van der Waals contacts. Voltage is converted into pressure waves, which create a cavitation field and microscopic bubbles. All of this will trigger the fibres to separate from one another. The same method was used in the present study to disperse GO and rGO in the cementitious composite. The solution was sonicated by ultrasonicator for 30 minutes to create the aqueous solution for the mortar mixes. After ultrasonication, GO/rGO is ready to be used with the mix for casting

3.3.3 Casting of Specimens

The moulds were thoroughly cleaned and lubricated before casting. Before casting, the screws were precisely tightened to the exact dimensions. before measuring GO and rGO, the beakers were thoroughly cleaned with acetone. The appropriate quantities of components were weighed for the design mix. For compressive strength along with piezo resistivity specimens, 50x50x50 mm moulds were employed. For flexural strength and electrical resistivity samples, 40x40x160mm moulds were used following (IS:4031-Part6).

The procedure of casting is as follows:

1. Along with cement, standard sand of three grades were precisely weighed.
2. For mixing, only clean equipment was utilized.
3. Cement and sand were dry mixed thoroughly for 60 seconds in a mortar mixer machine at low rpm.
4. Water, superplasticizer and GO for GO samples & rGO for rGO samples dispersed in liquid form were combined in a mortar mixer to get a homogenous mix.
5. Lastly, the mortar mixer was made to run for another 120 seconds at high rpm. Each batch's ingredients were prepared separately (**Figure 3.7**).

6. At each of the specified curing age, a minimum of three test samples must be prepared for testing
7. Curing ages ranging from 7 to 90 days were used for testing the specimens i.e., 7 days, 28 days, 56 days and 90 days.

Figure 3.7 Cube & Prism specimens after casting.

3.4 EXPERIMENTAL METHODS

Figure 3.8 shows the test matrix & methodology depicting varying dosages of GO & rGO along with the various properties which have been evaluated throughout the procedure.

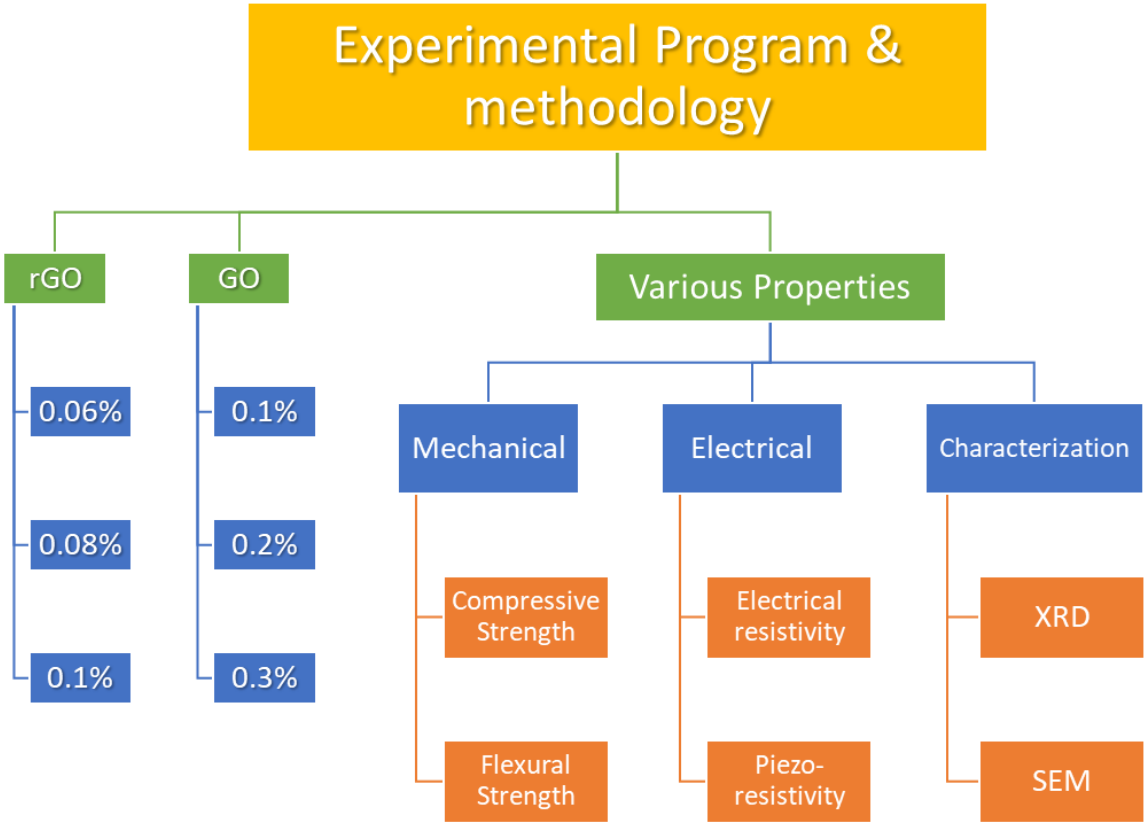

Figure 3.8 Schematic of research methodology.

3.4.1 Compression Strength Test (IS: 516-1959)

To determine the compressive strength of mortar cubes, the Compression test was performed at different curing ages of 7,28,56 and 90 days for both GO & rGO samples. During testing, samples were withdrawn from the curing tank and left to air dry for five to ten minutes. Compressive testing machine (CTM) was used to evaluate the samples at a loading rate of 0.1kN/s. The maximum capacity of CTM is 5000kN.

3.4.2 Flexural Strength Test (IS: 516-1959)

A flexure strength test was performed on mortar prisms to assess flexural strength at various curing ages. Without any packing, testing should be performed on their edges. For 7,28,56 and 90 days, the test should be performed for three prisms and the average value should be reported as the test result Flexure testing machine had a peak capacity of 100kN, the loading rate was set at 0.03kN/min.

3.4.3 Electrical Resistivity Test

A constant direct voltage (U) of 10 V was applied to the two probes by a power supply (DPS-305CF), and the current difference (I) was measured by a digital multi-meter connected to the stainless-steel electrodes (**Figure 3.9**).

The electrical resistance (R) of the sample was calculated by Ohm's law, **Equation 3.1**

$$R = U/I. \tag{3.1}$$

Considering that polarization is easily caused by ions (Ca^{2+}, OH^- etc.) in pore solution of cement-based composite under a direct current (DC) electric field, all specimens were first dried completely until weights were constant. The dried samples were then electrified for a certain amount of time (20 minutes) in order to further reduce the polarization effect before electrical tests (Wang and Zhang 2022). Electrical resistivity was calculated using **Equation 3.2.**

$$\rho = R\frac{A}{L} \tag{3.2}$$

where, ρ = Electrical resistivity**,** R = Resistance of the sample, L = Distance b/w two internal electrodes of the sample and A= Cross sectional area within electrodes.

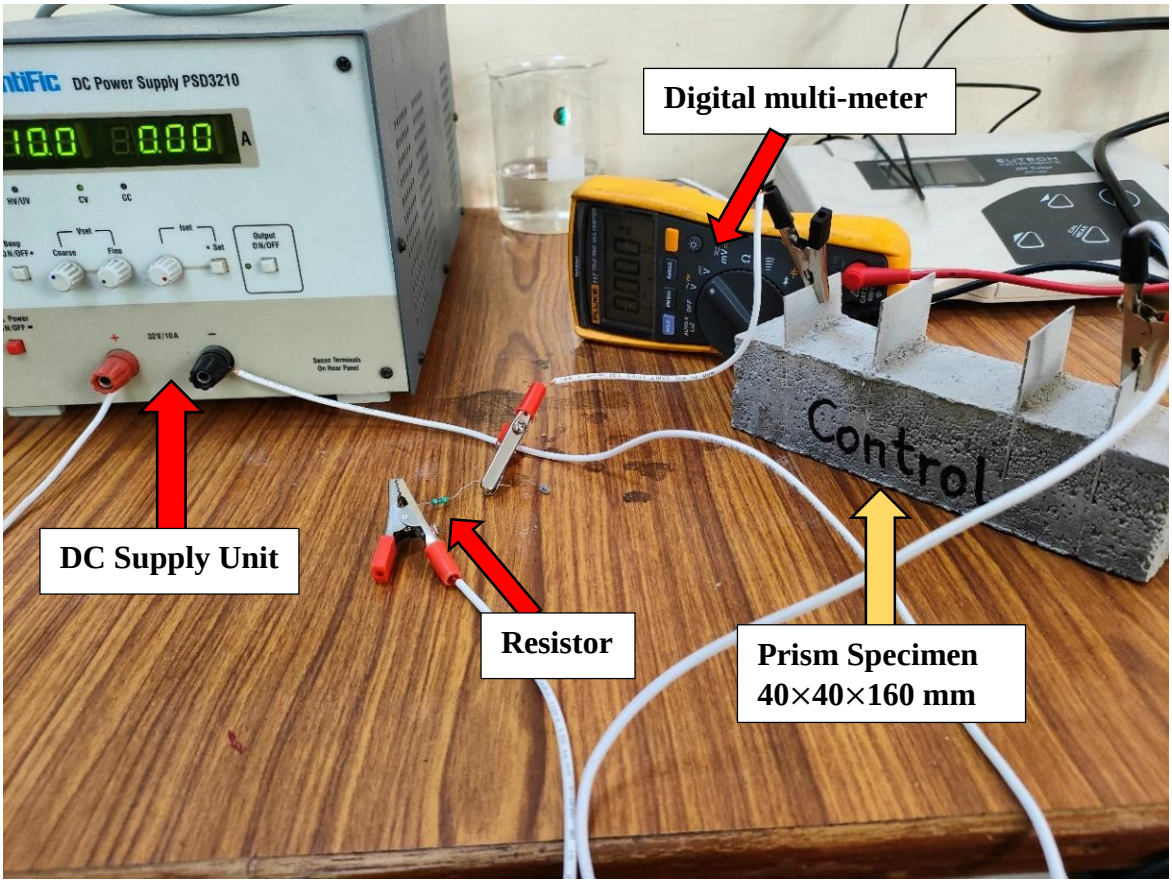

Figure 3.9 Setup for Electrical resistivity test

3.4.4 Piezo Resistivity Test

The piezo-resistivity of the composites was analysed by applying monotonic compressive loads and simultaneously measuring the deformation and electrical resistance (**Figure 3.11**). The piezoresistive sensitivity is usually evaluated by the gauge factor (GF), which can be defined as the fractional change of resistance (FCR) per strain unit sec. FCR is usually calculated in %. **Equation 3.3** was used to calculate FCR (Wang and Zhang 2022).

$$\text{FCR}\ (\%) = \frac{\rho_1 - \rho_0}{\rho_0} = \frac{\Delta\rho}{\rho_0} = \frac{\Delta R}{R} \qquad 3.3$$

Where, $\Delta\rho$ = change in resistivity (Ohm-m)

ρ_1 = resistivity after applying stress/strain and ρ_0 = initial resistivity.

ΔR = change in electrical resistance (Ohm)

R = initial electrical resistance (Ohm)

Experimental procedure followed for piezo-resistivity measurement was as follows:

1) Initially, the computer was connected with CTM and all the initial testing parameters (loading rate, specimen type, curing age, specimen dimensions) were assigned.
2) The next step included the wire-connection setup which had data logger, DC Supply unit, a resistor and plugs for plate (**Figure 3.11)**.
3) A 4-point electrode setup was used for piezo-resistivity measurement. A constant direct voltage (U) of 10 V was applied to the outer two stainless steel plate by a power supply (DPS-305CF), and the current difference (I) was measured by a data logger between the inner two steel plates.
4) After that, a command was given from the computer and compression loading was initiated.
5) Before initiating the test, the recording function on the data logger was switched on to store all the necessary data for recording the electrical resistivity.
6) Alongside the data logger, computer was recording a Force-time graph against the applied compressive stress until the specimen failed.
7) After the test, the recording function on the data was switched off and all the wired connections were removed for the next specimen.
8) Various parameters such as Area, length, Current, Voltage output for inner & outer plates were used to calculate resistivity (**Figure 3.10**).
9) After calculating resistivity, FCR was finally calculated using **Equation 3.3**.

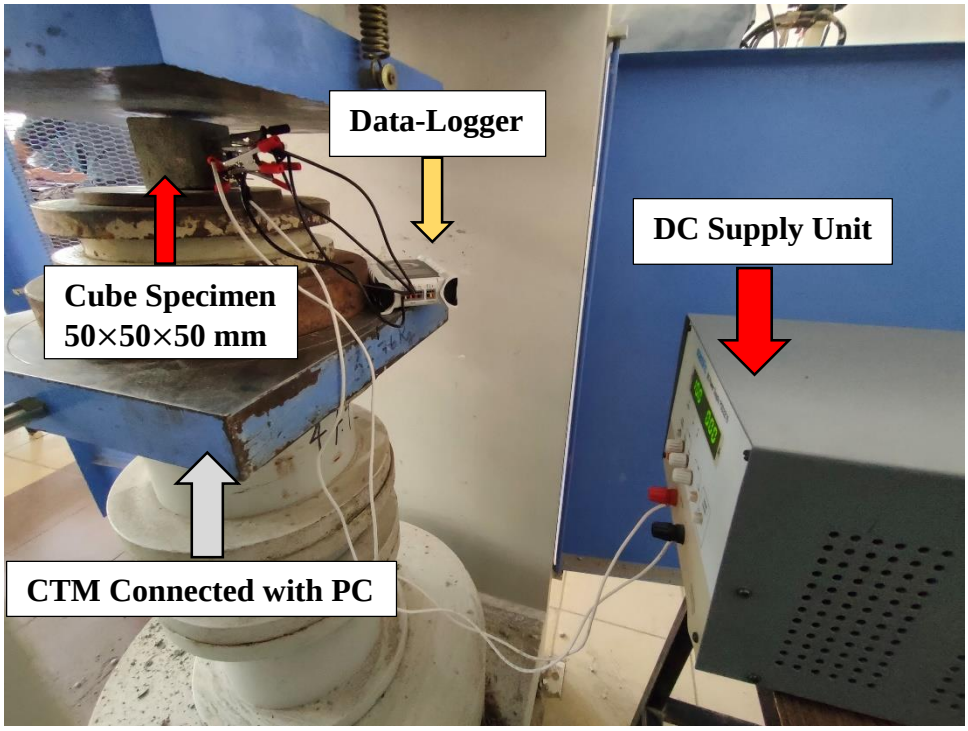

Figure 3.10 Setup for Piezo resistivity test

Time	Area (mm2)	Length (mm)	Resistor (ohm)	Outer plate (V)	Current (A)	Inner Plate (V)	Resistance (Ohms)	Resistivity (kohm cm)	FCR
0.5	2500	10	470	1.88394	0.004008	3.27165	816.202	20.405	0
1	2500	10	470	1.88384	0.004008	3.27167	816.250	20.406	0.00592
1.5	2500	10	470	1.88377	0.004008	3.27174	816.298	20.407	0.011776
2	2500	10	470	1.88384	0.004008	3.27167	816.250	20.406	0.00592
2.5	2500	10	470	1.88377	0.004008	3.27157	816.256	20.406	0.006579
3	2500	10	470	1.88381	0.004008	3.27166	816.261	20.407	0.007207
3.5	2500	10	470	1.88377	0.004008	3.27161	816.266	20.407	0.007802
4	2500	10	470	1.88387	0.004008	3.2715	816.195	20.405	-0.00087
4.5	2500	10	470	1.88376	0.004008	3.27151	816.245	20.406	0.005276
5	2500	10	470	1.88385	0.004008	3.27157	816.221	20.406	0.002332
5.5	2500	10	470	1.88379	0.004008	3.27151	816.232	20.406	0.003683

Figure 3.11 Screenshot of calculations of FCR in MS Excel

3.5 MICROSTRUCTURAL ANALYSIS

3.5.1 XRD

X-Ray Diffractometer (XRD) analysis with Cu- radiation was used to scrutinize the chemical properties of the specimens. In addition, 30kV and 40mV voltages were applied, with diffraction intensities ranging from 0°-90°.

3.5.2 SEM

Scanning Electron Microscopy (SEM) was used to investigate the microstructure of cementitious samples to discover variations in the microstructure due to addition of GO and rGO which led to an increase in piezo-resistivity of the composite.

3.6 SUMMARY

The experimental tests carried out were described in this chapter. Details of sample preparation and materials were presented. The experimental program was divided into two sections, which included evaluation of mechanical and electrical properties of cement-based GO and rGO specimens. Mechanical properties include tests of compressive strength and flexural strength. Whereas, electrical properties include tests for electrical resistivity and piezo-resistivity.

CHAPTER 4
RESULTS AND DISCUSSION

4.1 GENERAL

This chapter contains the findings of the experimental study. The numerous experimental tests that were carried out to determine changes in mechanical and electrical properties with the incorporation of GO & rGO in mortar samples were covered in the preceding chapter. This chapter discusses the performance of GO and rGO as self-sensing materials for RC structures. In this chapter, the results obtained are presented in full detail and the impact of GO & rGO are analysed.

4.2 COMPRESSIVE STRENGTH

4.2.1 Graphene Oxide

The change in the compressive strength of cementitious mix due to the addition of varying dosages of GO at different curing ages can be seen in **Figure 4.1**. On comparing with control mix, an increase in compressive strength was witnessed in all GO-M1, M2 & M3 specimens for 28 days curing age. But reduction of compressive strength with increased percentage of GO was also noticed for 28 & 56-days curing age.

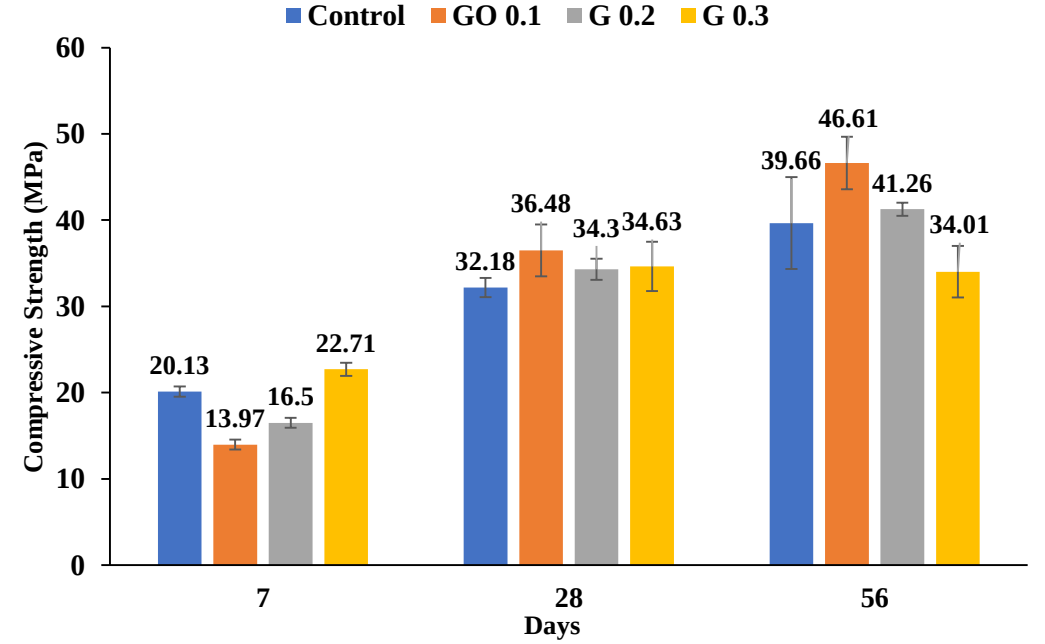

Figure 4.1 Compressive Strength results for GO cement-based specimens

This is mainly because of the influence of GO nanoparticle's oxygen-functional groups on the cementitious matrix which is associated with the reinforcing action on the mechanical properties of cementitious composites (Hou et al, 2017). The hydroxyl and carboxyl groups of GO and the mediating Ca^{2+} ions from calcium silicate hydrate of cementitious gels interact chemically to reinforce the structural strengths of GO cement-based specimens (Hou et al, 2017).

It can be observed that with an increase in the percentage of GO, compressive strength also increased at an early age of 7 days but as the curing age further increased the compressive strength started decreasing at 28 days and 56 days. The maximum compressive strength at 56 days was reported to be 46.61 MPa for GO M1 mix with 0.1% GO.

It was found that the compressive strength increased by 27.76% at 0.1% GO content at an age of 56 days as compared to 28 days of compressive strength. But, when the percentage of GO was increased from 0.1% to 0.3%, its compressive strength decreased by 5.34% for 28 days curing age and 37.04% for 56 days curing age **(Figure 4.2).**

GO 0.1% dosage content was found to be the most effective percentage for enhancing the compressive strength of GO cement-based composites. But as the dosage is increased from the optimum percentage, the reinforcing action between the cementitious matrix and GO's oxygen functional group fails due to agglomerations of GO particles at higher percentages (Pan et al, 2015). Consequently, it is unable to increase the compressive strength of the GO cement-based specimens for higher GO dosage.

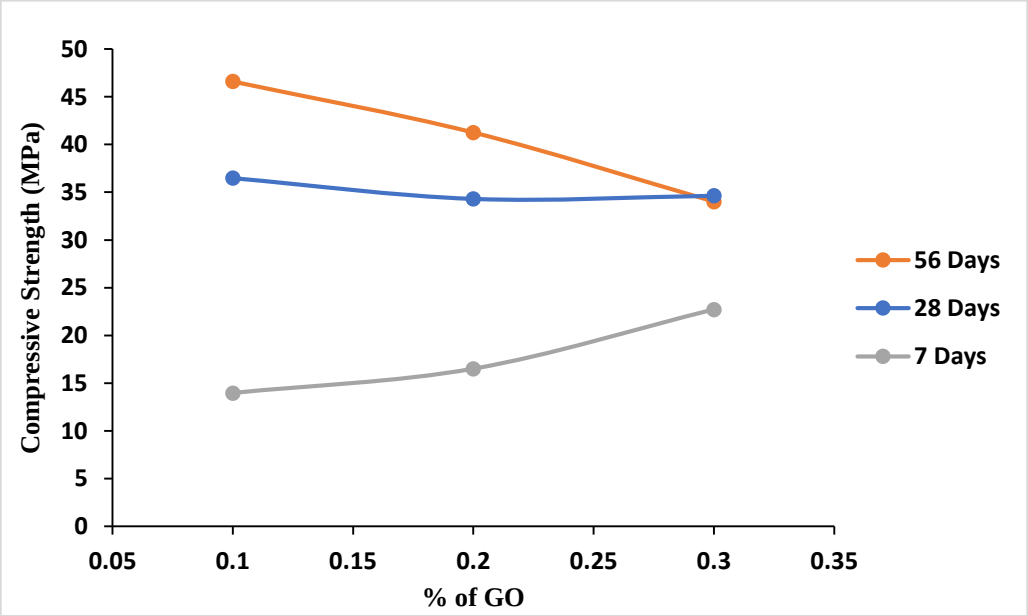

Figure 4.2 Change in compressive strength with change in % of GO dosage.

4.2.2 Reduced Graphene Oxide

In comparison with the control specimen, the compressive strength of 0.06%, 0.08% and 0.1% addition of rGO increased by 59.6%, 53.8% and 40% respectively at 7 days **(Figure 4.3).** However only 2% increase in strength is observed at 56 days for 0.08% addition of rGO. This increase in strength is mainly attributed to high physical strength of rGO (Qureshi and Paneshar 2019). Thus, for rGO specimens the increment in strength is higher in early age (7 days), compared to later age (28 days) in rGO based cementitious composites.

As the dosage increased, the compressive strength started decreasing at 7 days. The maximum compressive strength at 28 days was reported to be 32.9 MPa for rGO-M2. It was found that there was not much of a difference in comparing the compressive strength of the control mix & rGO specimens after 28 days of curing age. It was observed that there was a decrease of 7.76% compressive strength in the case of rGO-M1 when compared with the control mix at 28 days of compressive strength (**Figure 4.3**). This was mainly due to agglomerations of rGO nano-particles when added beyond 0.08%. Due to hydrophobic nature of rGO, its inclusion in cementitious matrix may significantly decrease the degree of water penetration at higher percentages. Due to the increased rGO dosages employed, rGO aggregated which prevented rGO from interacting with the cement matrix (Du and Pang, 2015).

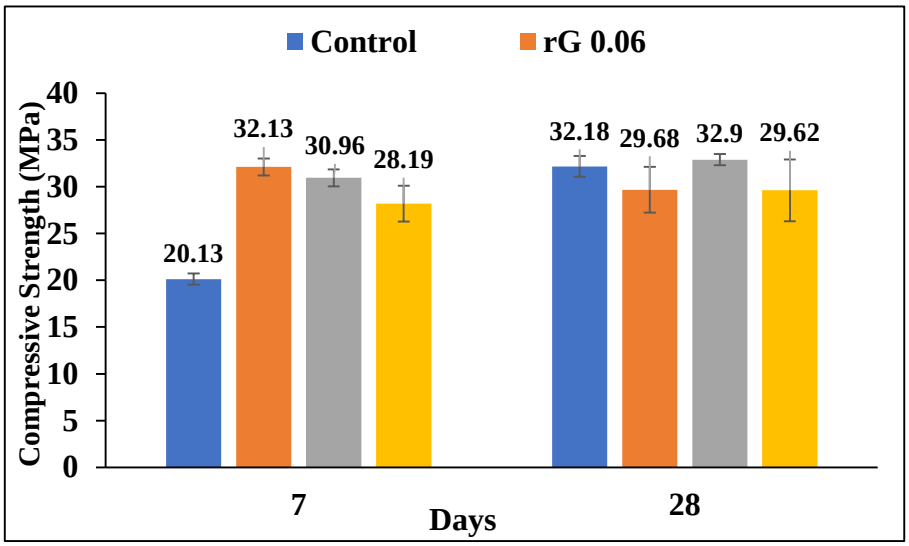

Figure 4.3 Compressive Strength results for rGO cement-based specimens

4.3 FLEXURAL STRENGTH

4.3.1 Graphene Oxide

The result of flexural strength for varying dosages of GO at different curing ages can be seen in the **Figure 4.4**. Similar to compressive strength, mixes with GO showed increased flexural strength compared to the control mix.

GO increased in the percentage of GO, increased flexural strength. The maximum strength is achieved for GO-M3 mix, which showed 27% increase in flexural strength compared to control mix at 28 days and 10% increase at 56 days. Due to presence of higher number of functional groups on the surface and periphery of graphene layers in case of GO, stronger adhesion bonds are formed between GO and cement matrix due to its reaction with cement hydration products, resulting in higher strength (Qureshi and Paneshar 2019).

It was found that GO-M3 was the optimum percentage for enhancing flexural strength for GO cement-based specimens.

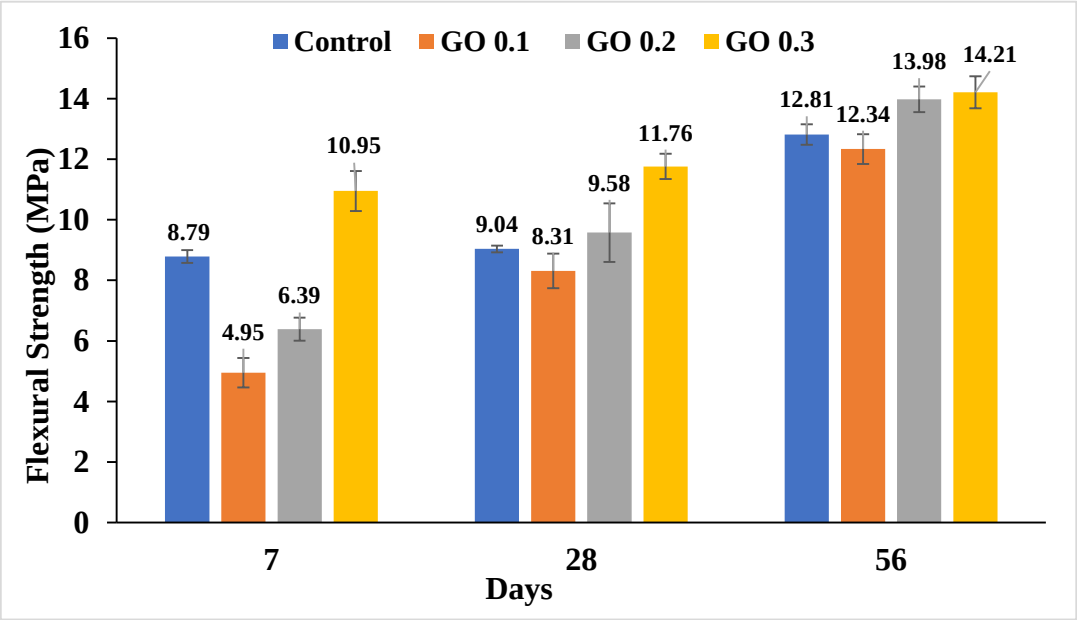

Figure 4.4 Flexural Strength results for GO cement-based specimens

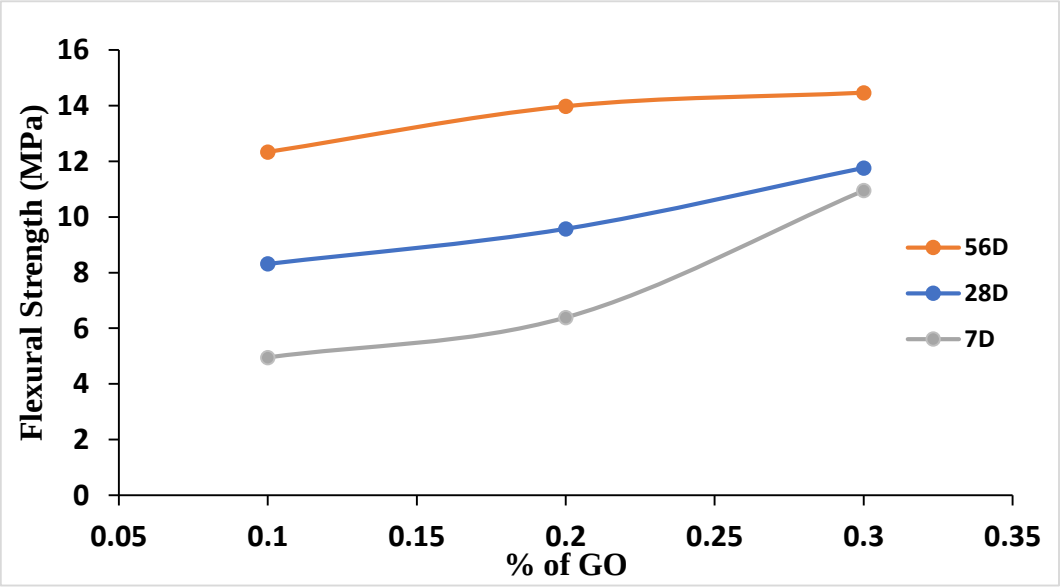

Figure 4.5 Change in flexural strength with change in % of GO dosage.

4.3.2 Reduced Graphene Oxide

Results for flexural strength show a decrease in flexural strength with an increasing percentage of rGO. On comparing rGO-M1 at 7- days and 28-day curing age, an increase of 19.17% flexural strength was noticed. The maximum flexural strength was reported to be 11.5 MPa for rGO-M1 after 28 days of curing age. But, as the rGO percentage increased from 0.06% to 0.1%, a decrease of 17.34% was found in the case of 28 days of flexural strength (**Figure 4.6**).

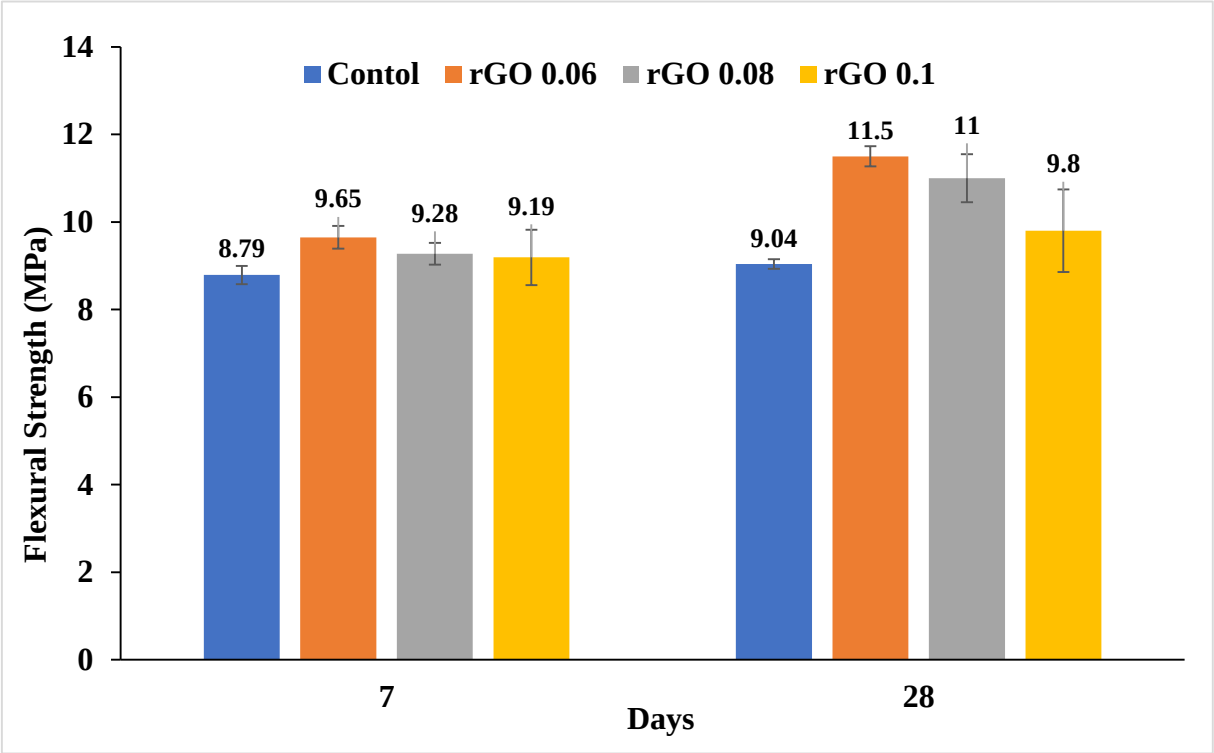

Figure 4.6 Flexural Strength results for rGO cement-based specimens

rGO-M1 was reported to be the best among other dosage content to enhance the flexural strength of rGO cement-based specimens. Flexural strength declines monotonically and consistently as the rGO content rises over 0.06%. This might be due to the decreased degree of water penetration at a higher dosage of rGO which makes the rGO nano-particles aggregated and prevents them to interact with the cement matrix.

On comparing the compressive strengths of GO and rGO specimens, it was observed that for 28 days curing age, GO-M1 showed maximum strength (36.48 MPa) among all the specimens.

4.4 ELECTRICAL RESISTIVITY

It can be seen in **Figure 4.7 & 4.8** that electrical resistivity increased with an increase in curing age as compared to the control specimen. An electrical resistivity test was conducted using a 4-probe method. Since the plates embedded in the prism specimen were of the exact size as

that of the mould dimensions i.e., 40×60×1mm. The connection between the cement matrix and plates was not proper. Thus, giving improper electrical resistivity results.

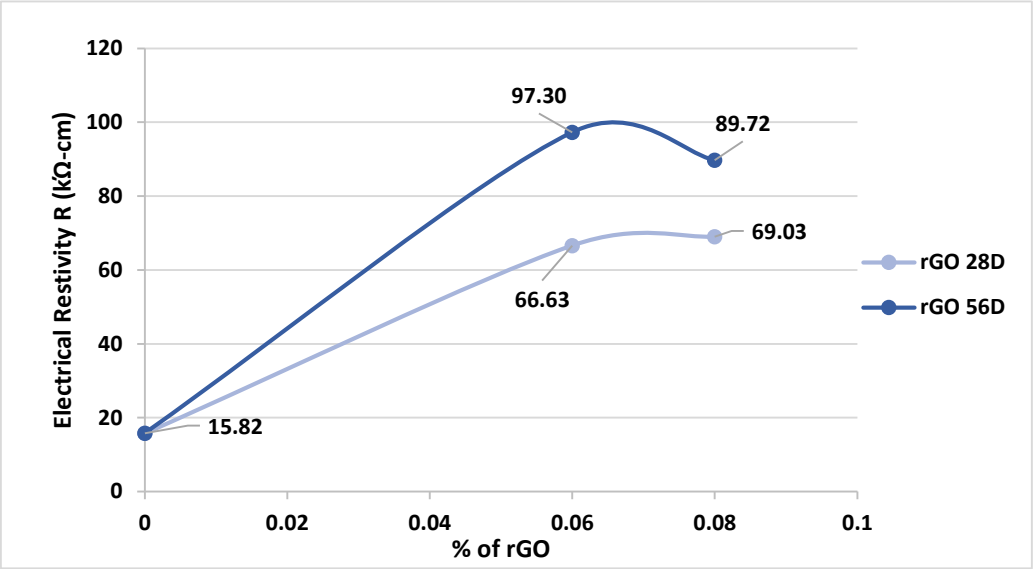

Figure 4.7 Electrical Resistivity of rGO Specimens

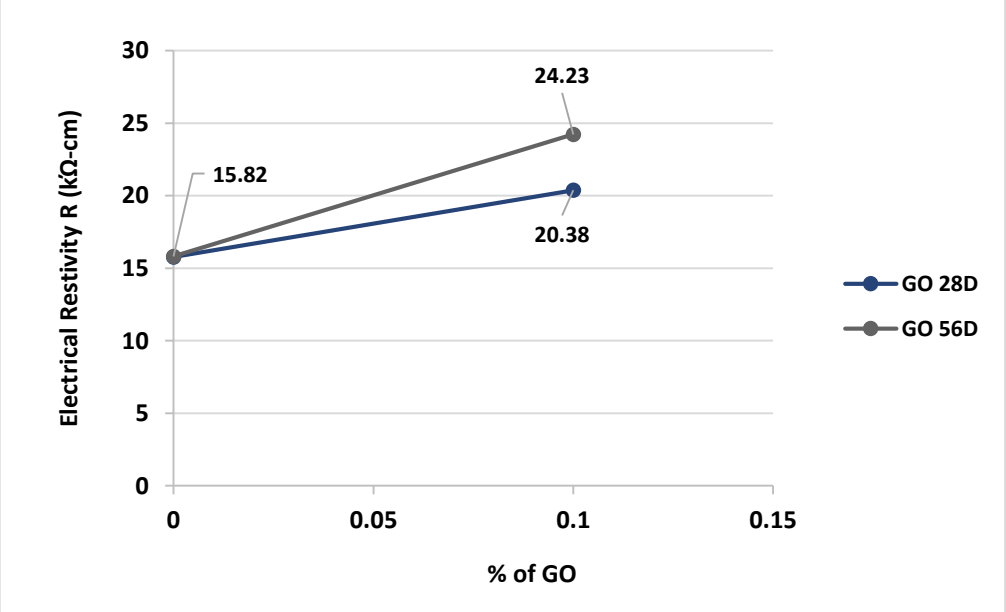

Figure 4.8 Electrical resistivity of GO Specimens

4.5 PIEZO RESISTIVITY

Time history relationships between compressive stress and FCR of control mix at 28 days curing under monotonic compression from loading to failure are shown in **Figure 4.9**. It can be seen that the FCR of the specimen remains constant throughout with increasing compressive stress. The absolute maximum FCR of the Control mix is 0% respectively. The maximum stress value of the control mix for 28 days and 56 days was found to be 30.8 MPa and 52.8 MPa, respectively (**Figure 4.10**). No stress sensitivity was found in the control specimen till 56 days of curing age.

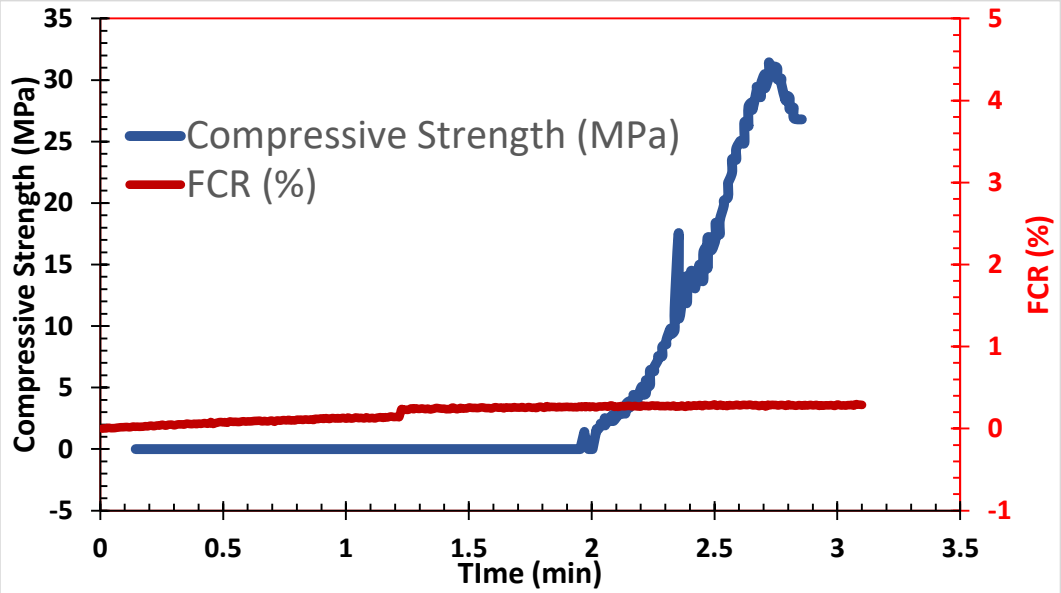

Figure 4.9 FCR vs Compressive stress for Control mix (28 days)

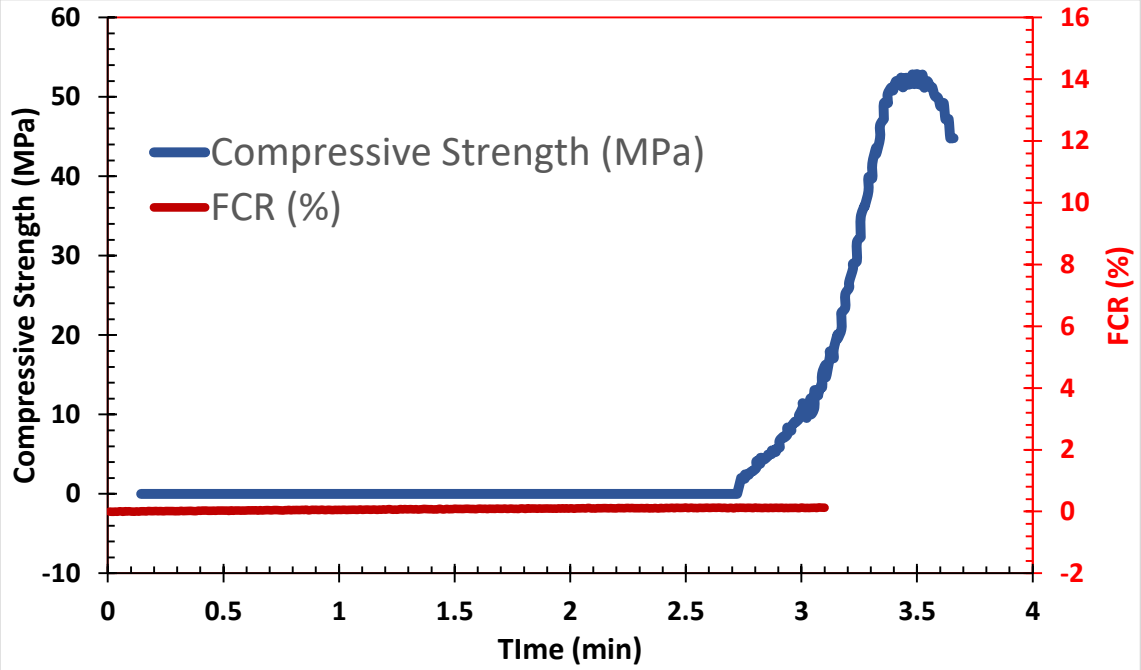

Figure 4.10 FCR vs Compressive stress for Control mix (56 days)

4.5.1 Graphene Oxide

Time history relationships between FCR and monotonic compressive stress of GO-0.1,0.2 and 0.3% at the curing age of 28 days are shown in **Figures 4.12, 4.13 & 4.14**, respectively. FCR decreases with increasing stress and increases with decreasing stress. FCR increases gradually as stress increases to the ultimate value, and then the specimen is failed. Therefore, the stress states of specimens can be evaluated by these characteristics.

The maximum absolute FCR among all three percentages of GO at 28 days is for GO-M3 which is 54.6% at a maximum stress value of 44.8 MPa (**Figure 4.12**). Whereas, GO-M1 and GO-M2 show absolute FCR values of 31.86% and 12.86%at maximum stress values of 36.64 MPa and 37.28 MPa respectively. But, GO-M1 at 56 days (**Figure 4.11**) showed maximum absolute FCR as 50.69% at a maximum stress value of 64.8 MPa. The stress sensitivities of 0.1%, 0.2% and 0.3% were reported as 0.8677, 0.344 and 1.166 respectively

The formation of conductive networks between cement matrix with uniformly dispersed nanofiller is the main cause for increased sensitivity. Better conductive networks allow electrical current pass more easily through the composite which helps in getting better sensitivity results. GO-M1 specimens showed better sensitivity results, since GO-M1 was more easily dispersed as compared to GO-M2 & GO-M3.

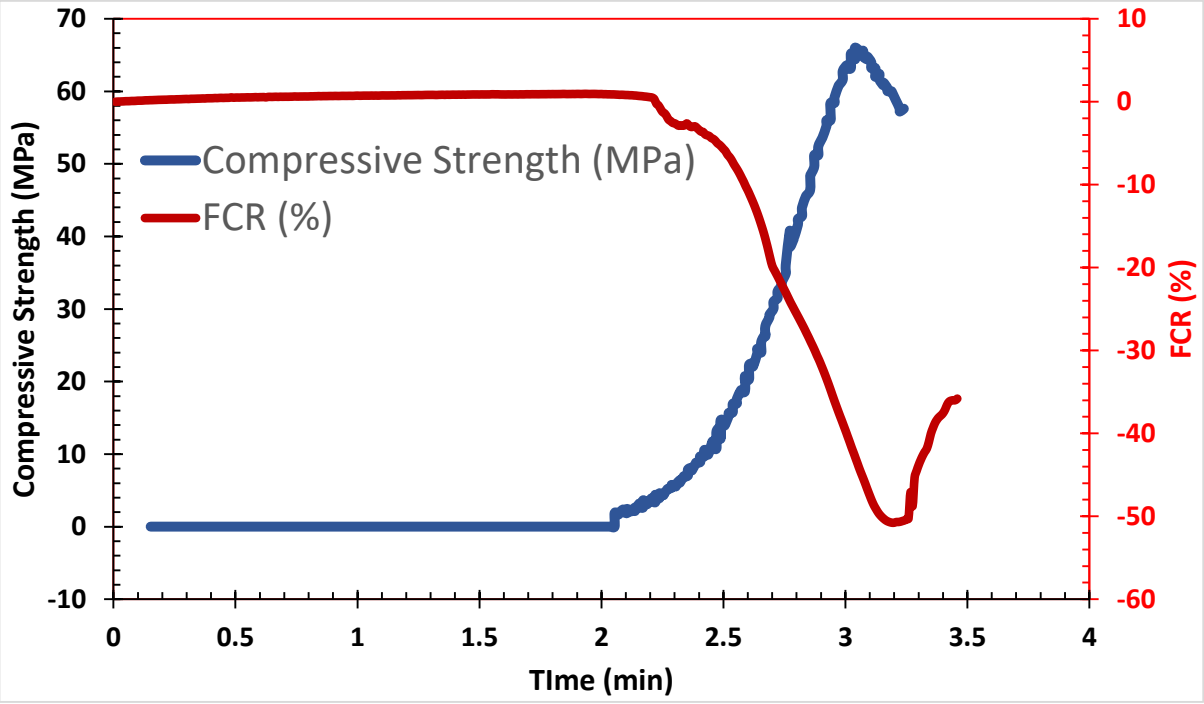

Figure 4.11 FCR vs Compressive stress for GO 0.1% (56 days)

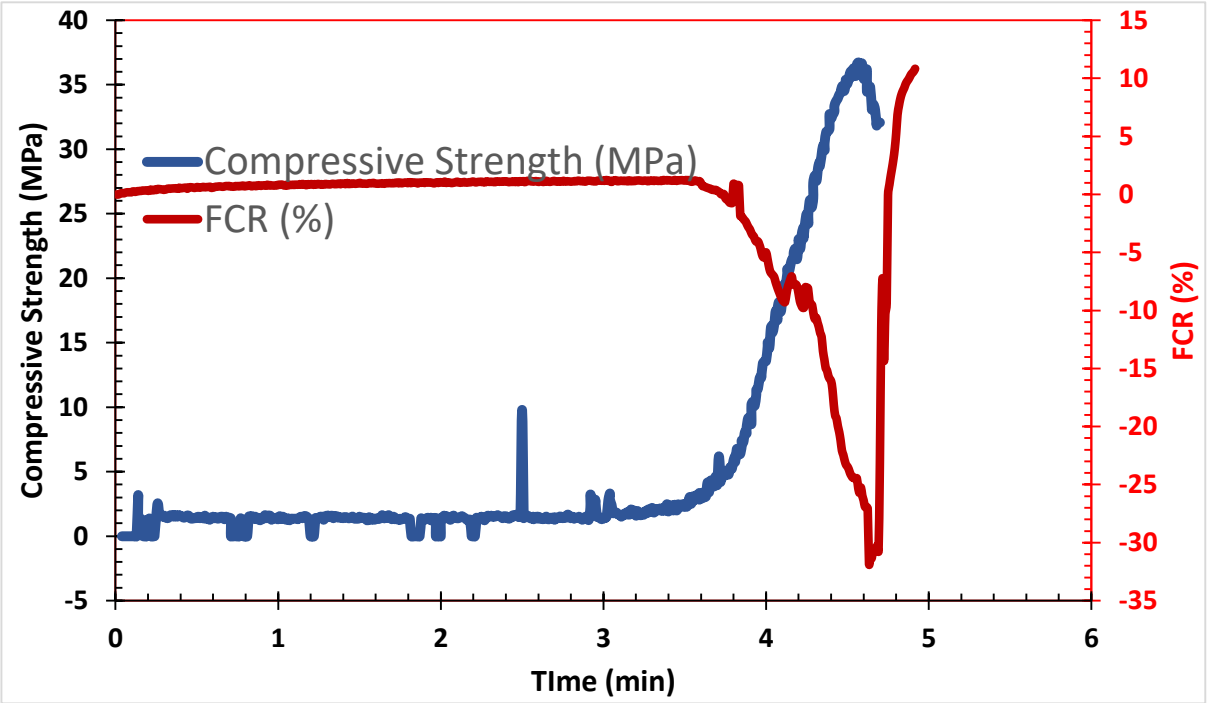

Figure 4.12 FCR vs Compressive stress for GO 0.1% (28 days)

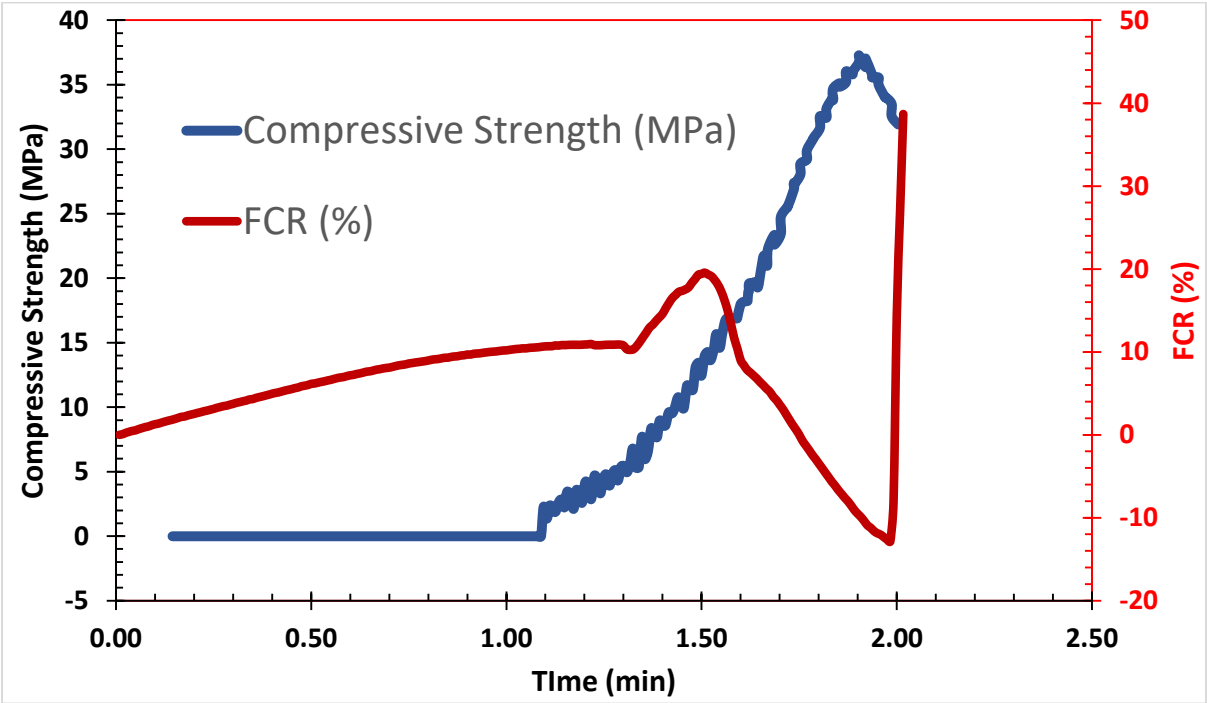

Figure 4.13 FCR vs Compressive stress for GO 0.2% (28 days)

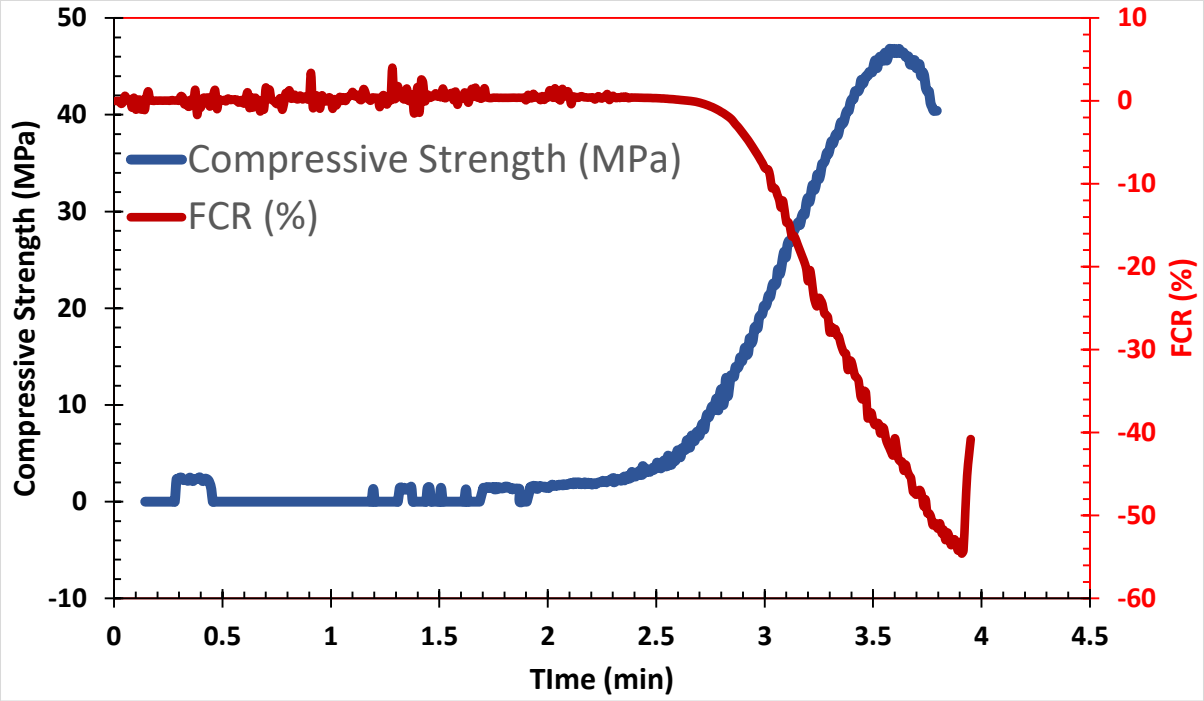

Figure 4.14 FCR vs Compressive stress for GO 0.3% (28 days)

The results present good repeatability and stability. As can be seen from **Figures 4.15, 4.16 & 4.17**. The fitness of FCR and stress for GO 0.1%,0.2% and 0.3% was found to be 0.9691, 0.6104 and 0.9946, respectively.

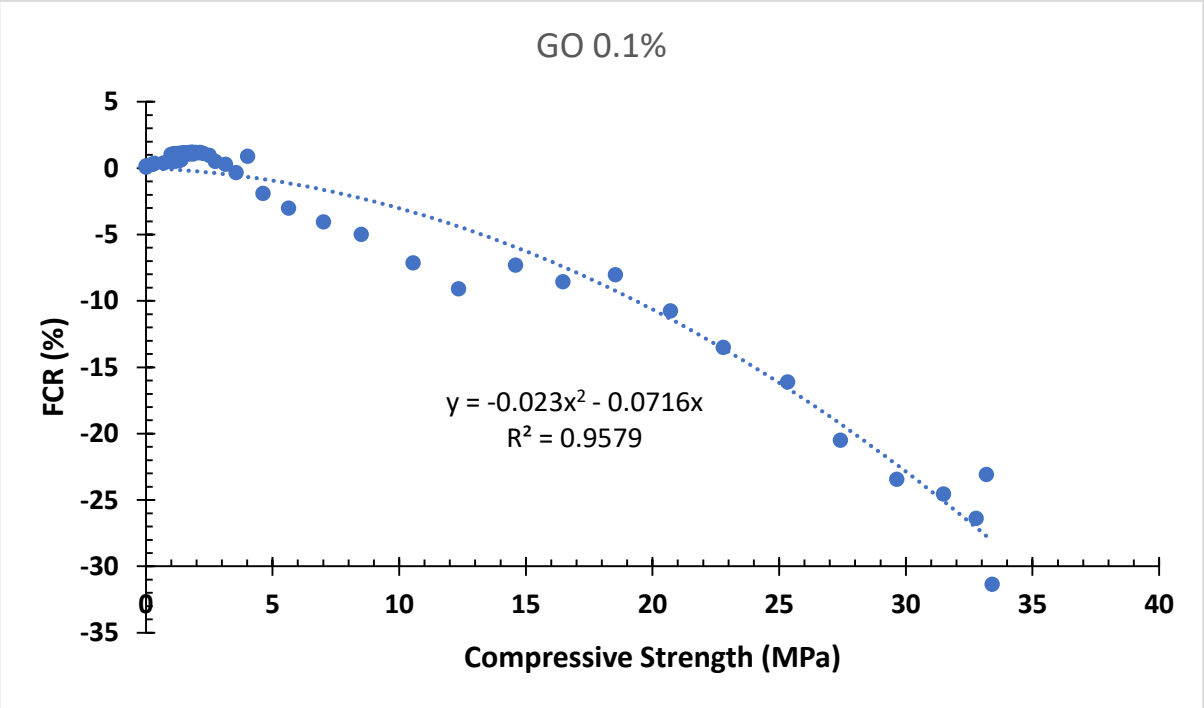

Figure 4.15 Fitting curve between FCR and Compressive strength for GO 0.1%

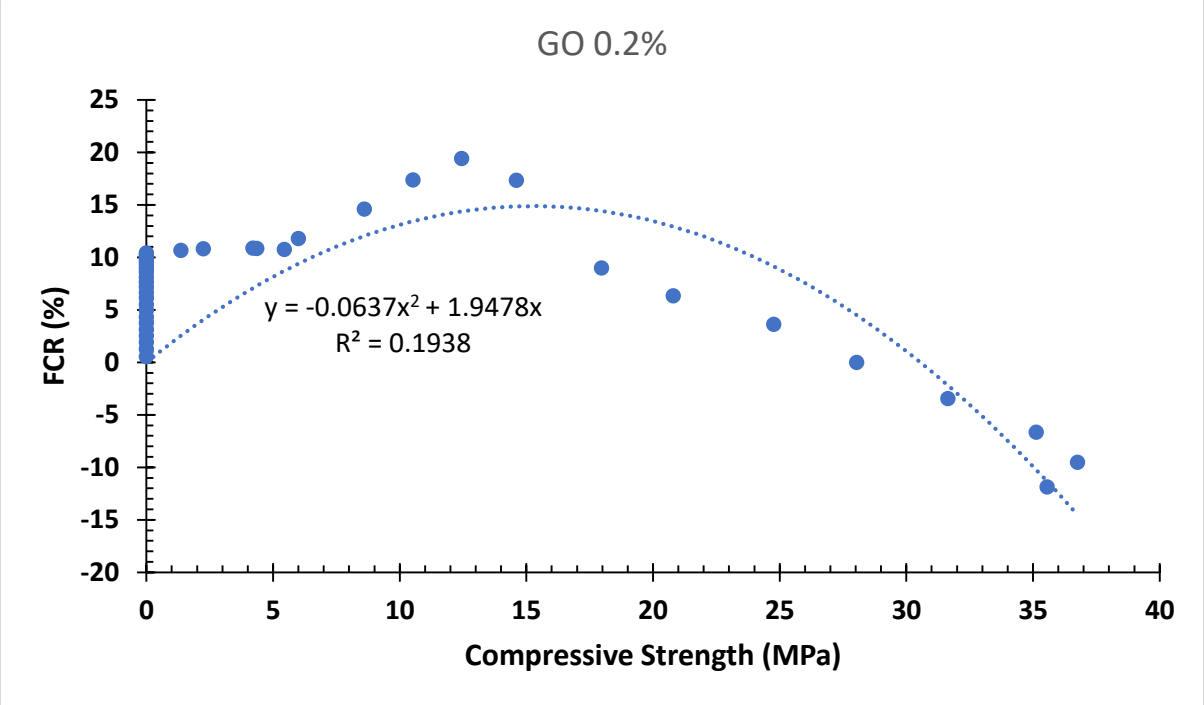

Figure 4.16 Fitting curve between FCR and Compressive strength for GO 0.2%

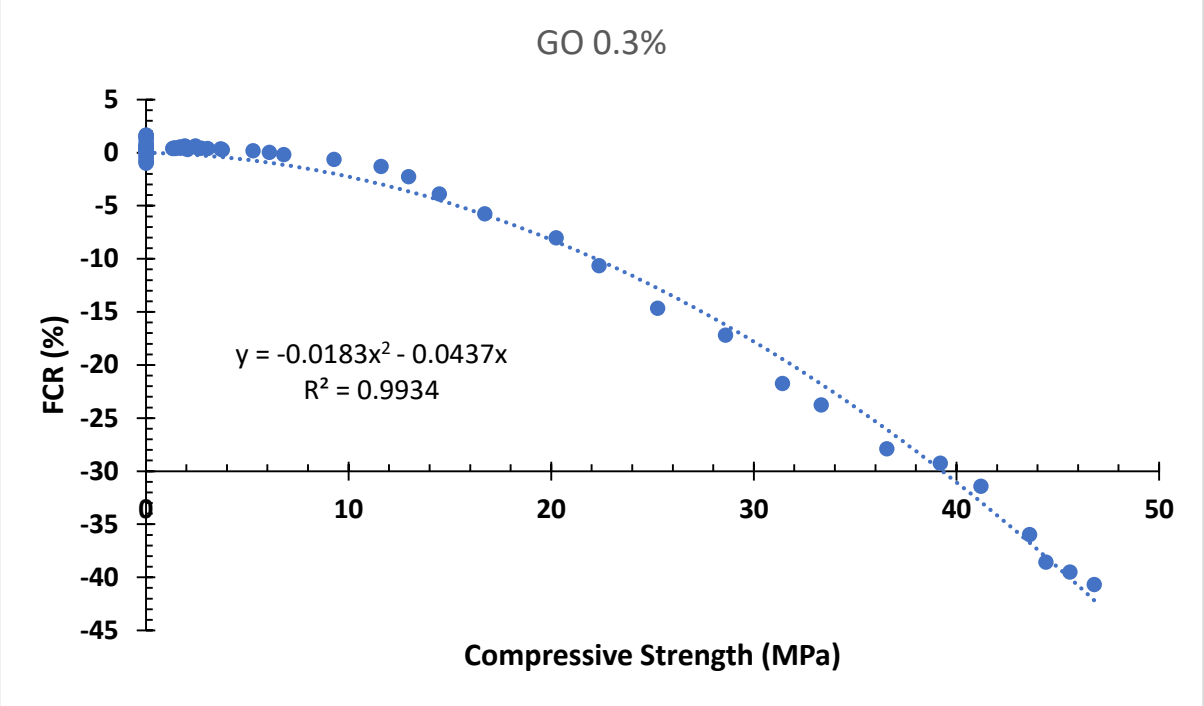

Figure 4.17 Fitting curve between FCR and Compressive strength for GO 0.3%

4.5.2 Reduced Graphene Oxide

Meanwhile, relationships between FCR and monotonic stress of rGO are better than GO specimens. Correspondingly, the percentages of rGO comparatively to that of GO were lowered down to 0.06%, 0.08% and 0.1% respectively. The sensor's FCR may be split into two phases, the first of which is from the start of loading to the sensor's maximum compressive stress. During this stage, the sensor's FCR drops as the compressive stress increases, and there is a strong correlation between these two parameters. After attaining the maximum stress, the specimen failed and the load suddenly dropped, so does the FCR. This shows that rGO based cement specimens are sensitive to loading (Ding et al, 2019).

The findings show that among the three percentages of rGO 28 days, the maximum absolute FCR is from rGO-M1 which is 56.81% at a maximum stress level of 25.68 MPa respectively (**Figure 4.18**). Whereas, rGO-M2 (**Figure 4.19)** and rGO-M3 (**Figure 4.20**) show the maximum FCR values as 47.31% and 42.84% at maximum stress values of 34.08 MPa and 32.92 MPa respectively. This is due to the formation of uniformly distributed rGO conductive networks within the composites (Saafi et al, 2014).

The stress sensitivities of 0.0.6%, 0.08% and 0.1% were reported as 2.1784, 1.366 and 1.0501 respectively. Therefore, comparing the results of stress sensitivities between GO and rGO, we scan observe that there is an increase of 21% of rGO-M1 as compared to that of GO-M1. The

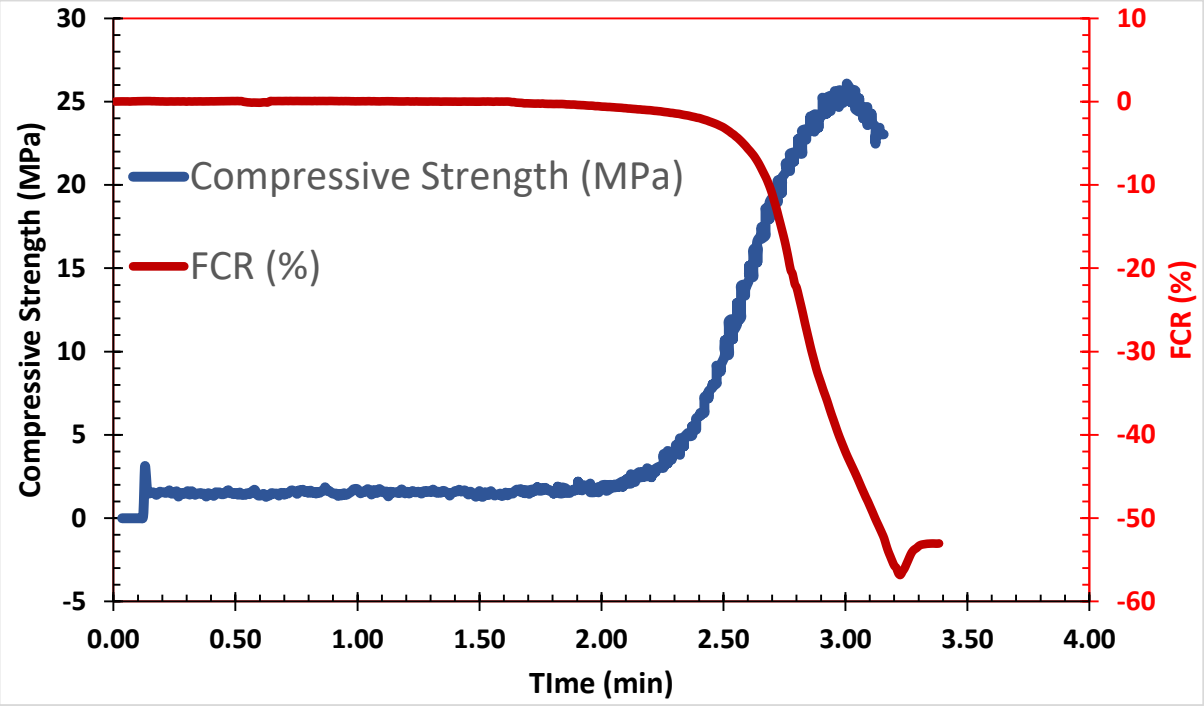

Figure 4.18 FCR vs Compressive stress for rGO 0.06% (28 days)

sensitivity increases with the fiber content's proximity to the percolation threshold and the quality of the fiber dispersion (Sun et al, 2015). Since rGO 0.06% was more easily dispersed than higher concentrations, that is the reason rGO-M1 was able to provide much higher sensitivity.

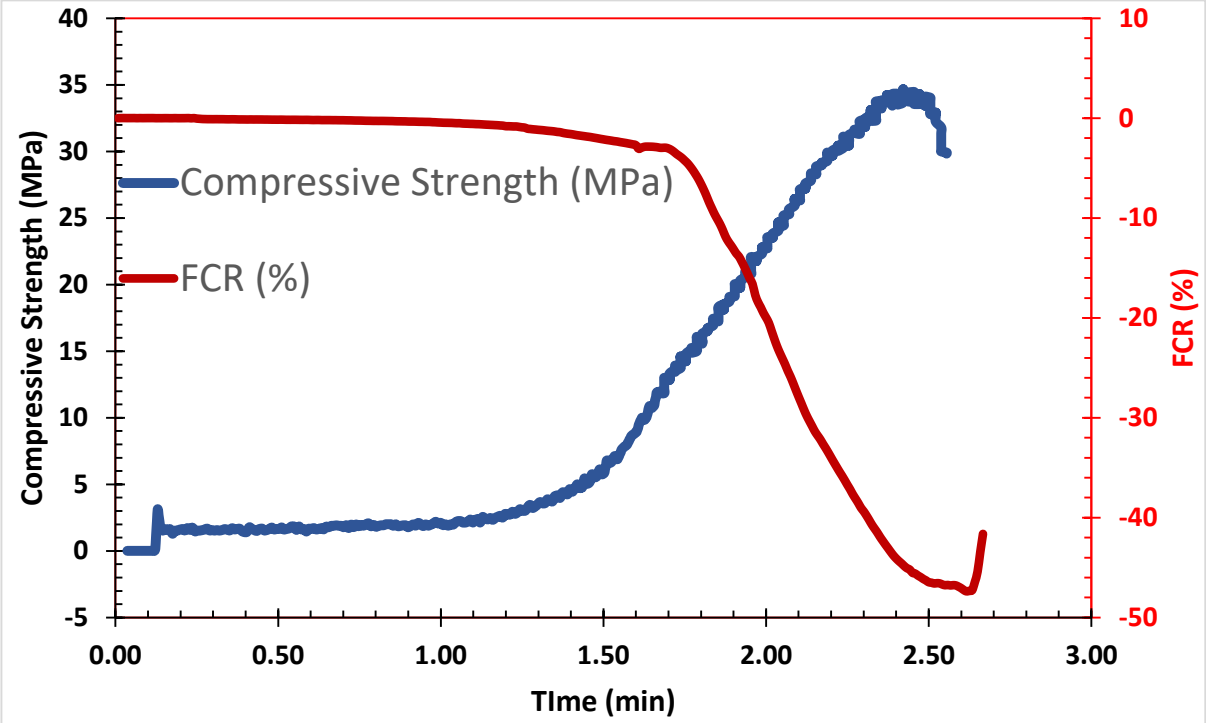

Figure 4.19 FCR vs Compressive stress for rGO 0.08% (28 days)

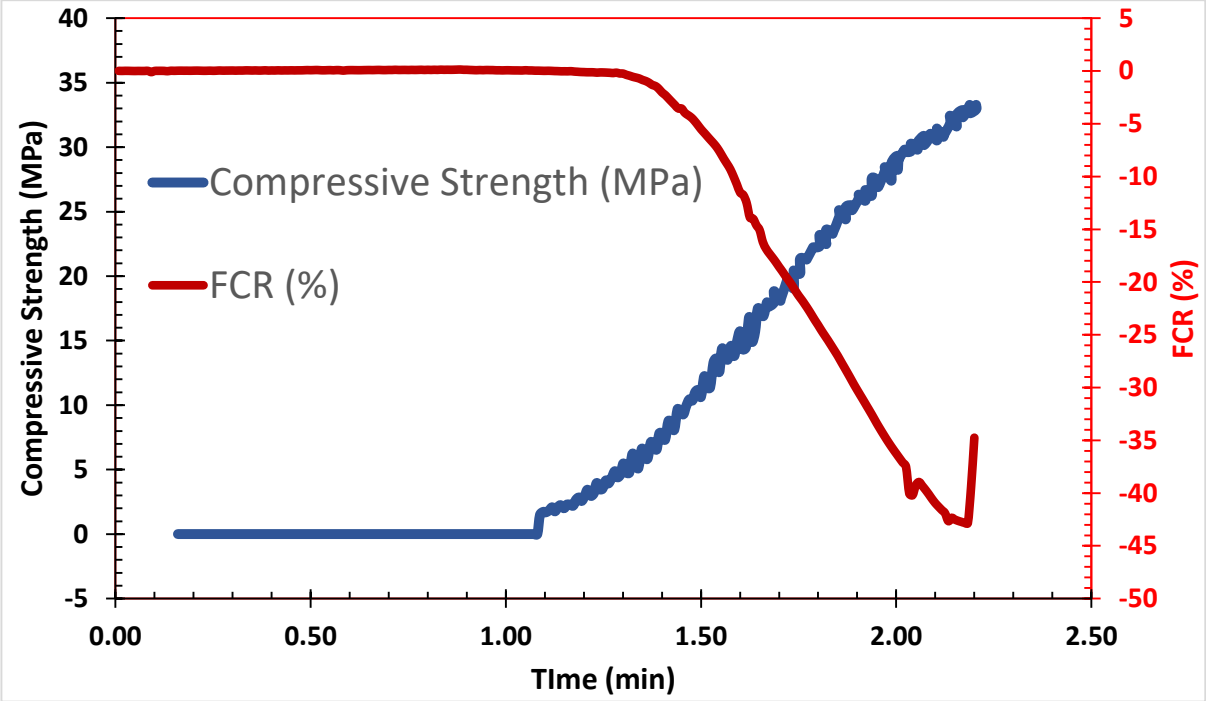

Figure 4.20 FCR vs Compressive stress for rGO 0.1% (28 days)

The repeatability and stability of the results are good as seen in **Figures 4.21, 4.22 & 4.23**. The fitness of FCR and stress for rGO 0.06%, 0.08% and 0.1% was found to be 0.9564, 0.9948 and 0.9961, respectively.

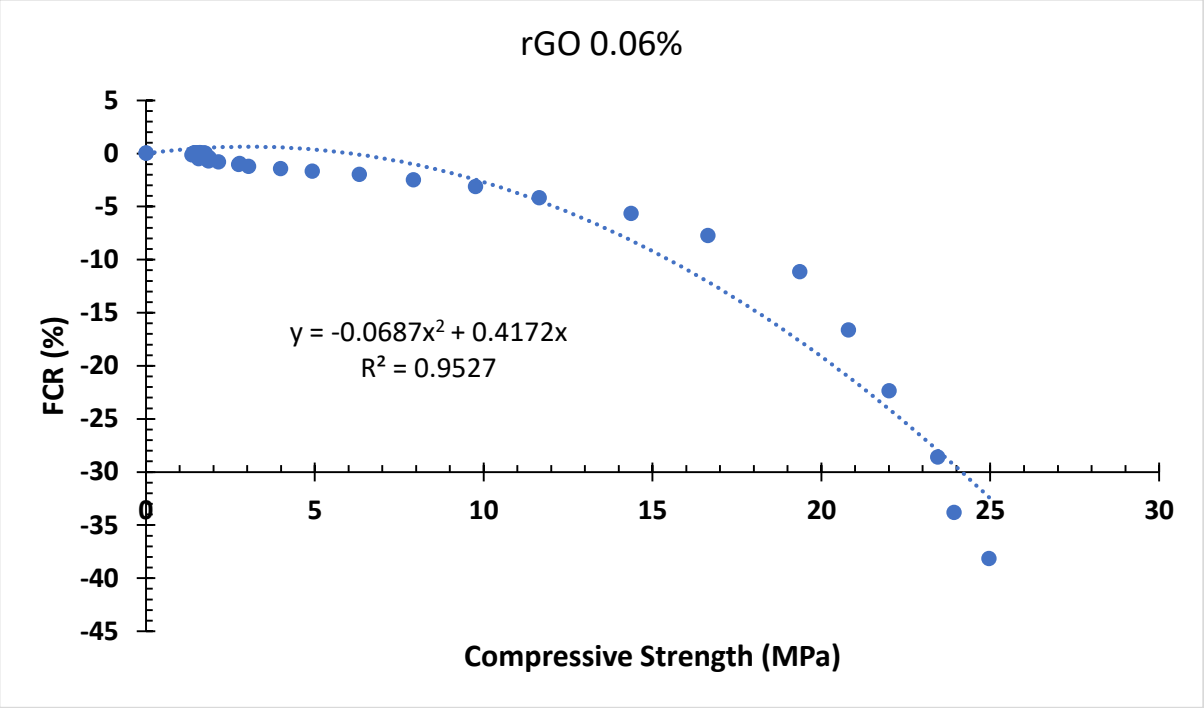

Figure 4.21 Fitting curve between FCR and Compressive strength for rGO 0.06%

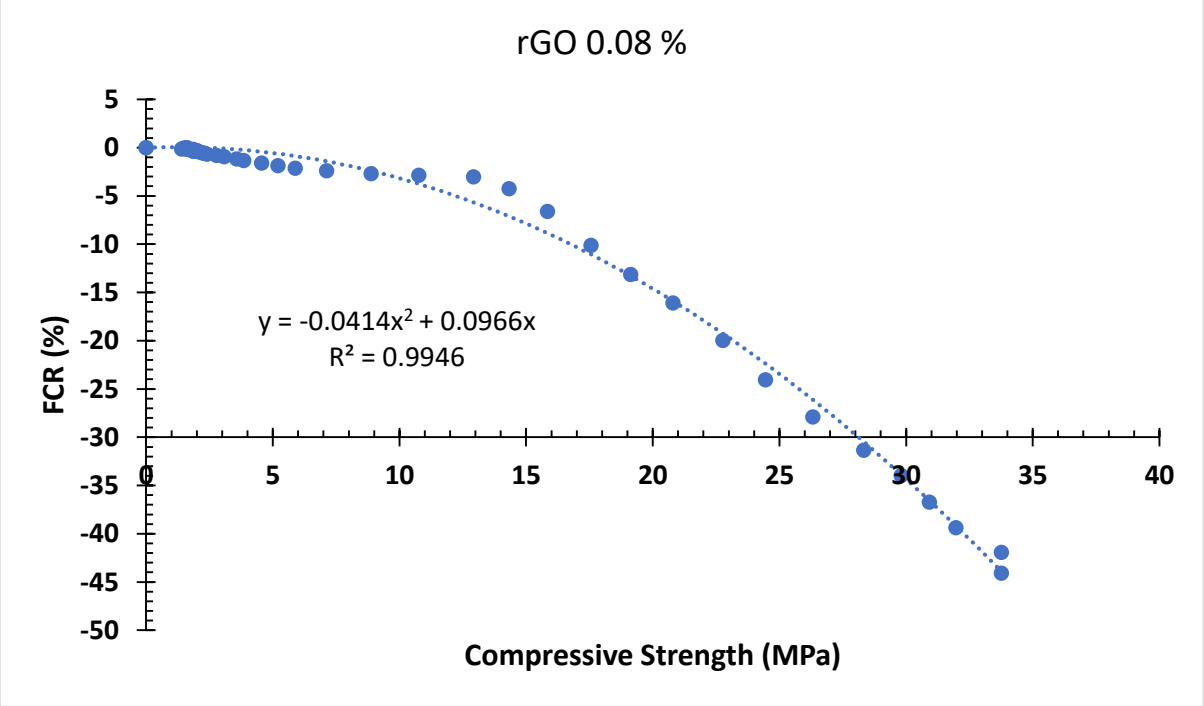

Figure 4.22 Fitting curve between FCR and Compressive strength for rGO 0.08%

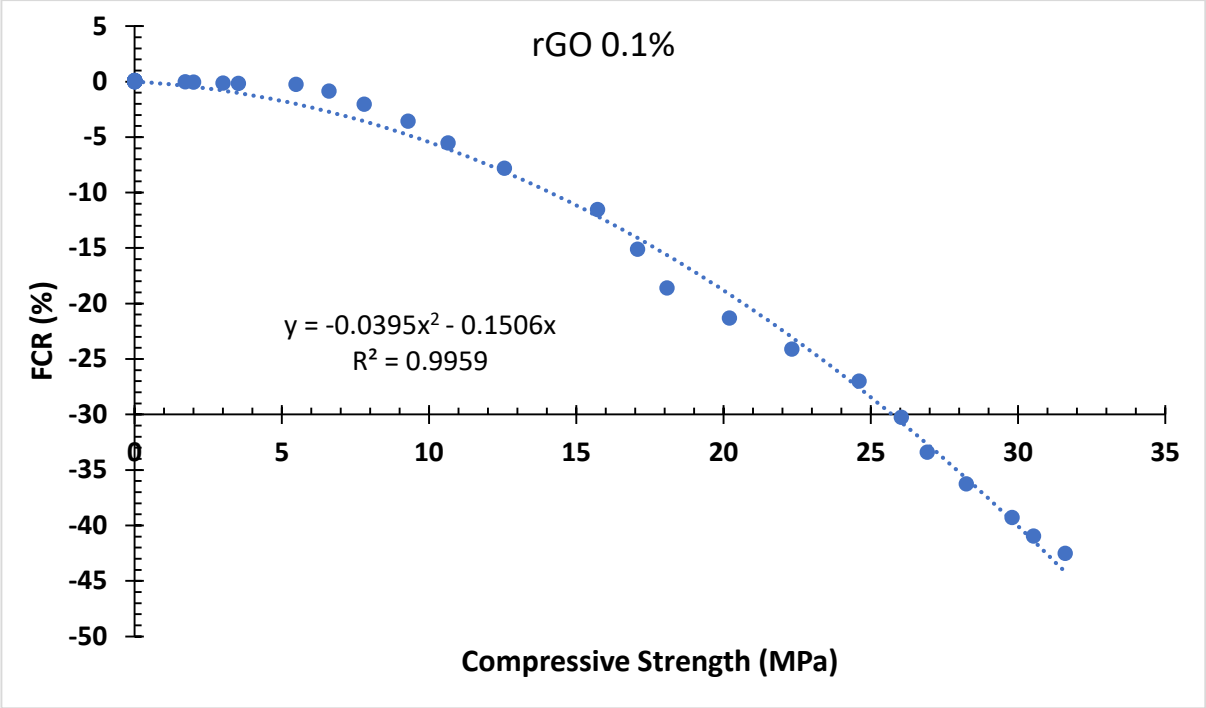

Figure 4.23 Fitting curve between FCR and Compressive strength for rGO 0.1%

On comparing all the stress sensitivities of all the varying percentages of GO 0.1%, 0.2% & 0.3% and rGO ranging from 0.06%, 0.08% & 0.1%, the maximum sensitivity value was found to be in the case of rGO-0.06%, which is 2.1784 (**Figure 4.24**).

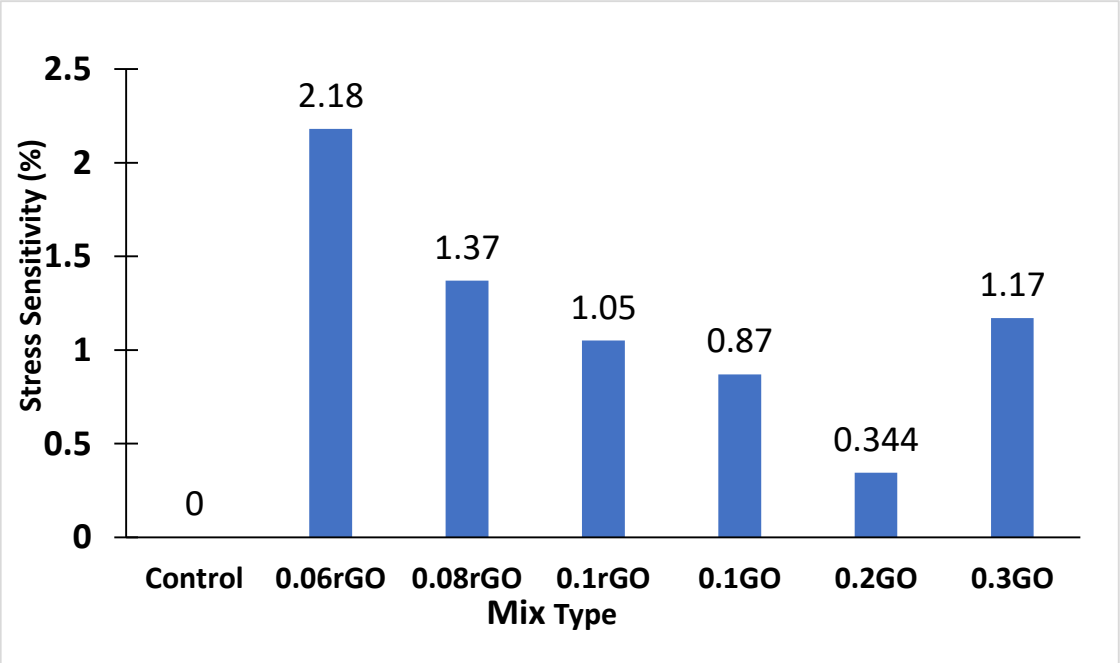

Figure 4.24 Stress sensitivities of rGO and GO specimens.

4.6 MICROSTRUCTURAL IMAGE ANALYSIS

As can be seen from **Figure 4.25**, it can be observed that microstructure of cementitious mortar (Fig (a) and (b)) got densified by addition of 0.1% GO (Fig (c) and (d)) and 0.06% rGO (Fig (e) and (f)). This confirms, the pore filling nature of the composites. Further in GO-M1 mix, at few locations agglomeration of GO can also be observed, this leads to pore refinement, hence increase in the mechanical properties. High water dispersibility and small pore size of GO, leads to pore refinement nature of GO (Qureshi and Paneshar 2019). Further increase in GO concentration, leads to enhance agglomeration, hence reduction in compressive strength.

Compared to GO, in rGO specimens, cluster of rGO is more randomly distributed, this is attributed to lower surface area of rGO, compared to GO. Thus, denser microstructure was observed in rGO-M1 mix compared to control, which indicates micro-crack bridging (Madbouly et al. 2020). The main hydration products seen in the pores of rGO composites were ettringites.

The SEM images of GO-M1 and rGO-M1 mix depicts that GO and rGO have reinforced the microstructure of cementitious mortar. However, pore filling nature of GO composite is more homogeneous compared to random pore filling in rGO, leading to more porous microstructure in rGO compared to GO mix. Moreover, due to presence of more hydroxyl and carboxyl functional groups in GO leads to higher production rate of C-S-H and CH, leading to higher strength in GO composites compared to rGO composites (Qureshi and Paneshar 2019).

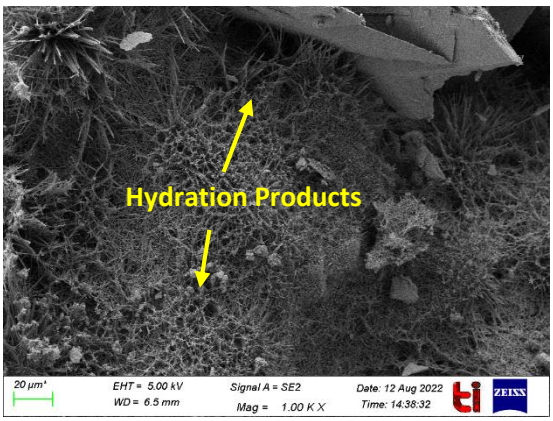

(a)

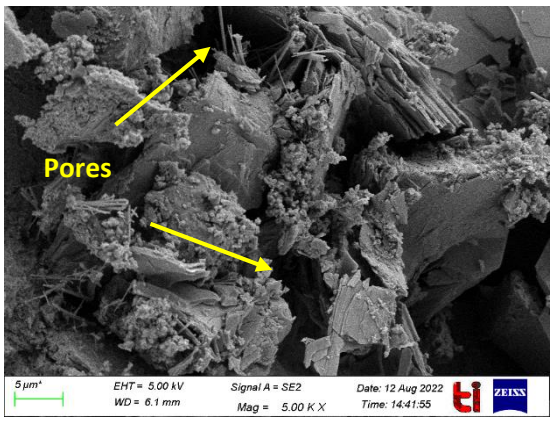

(b)

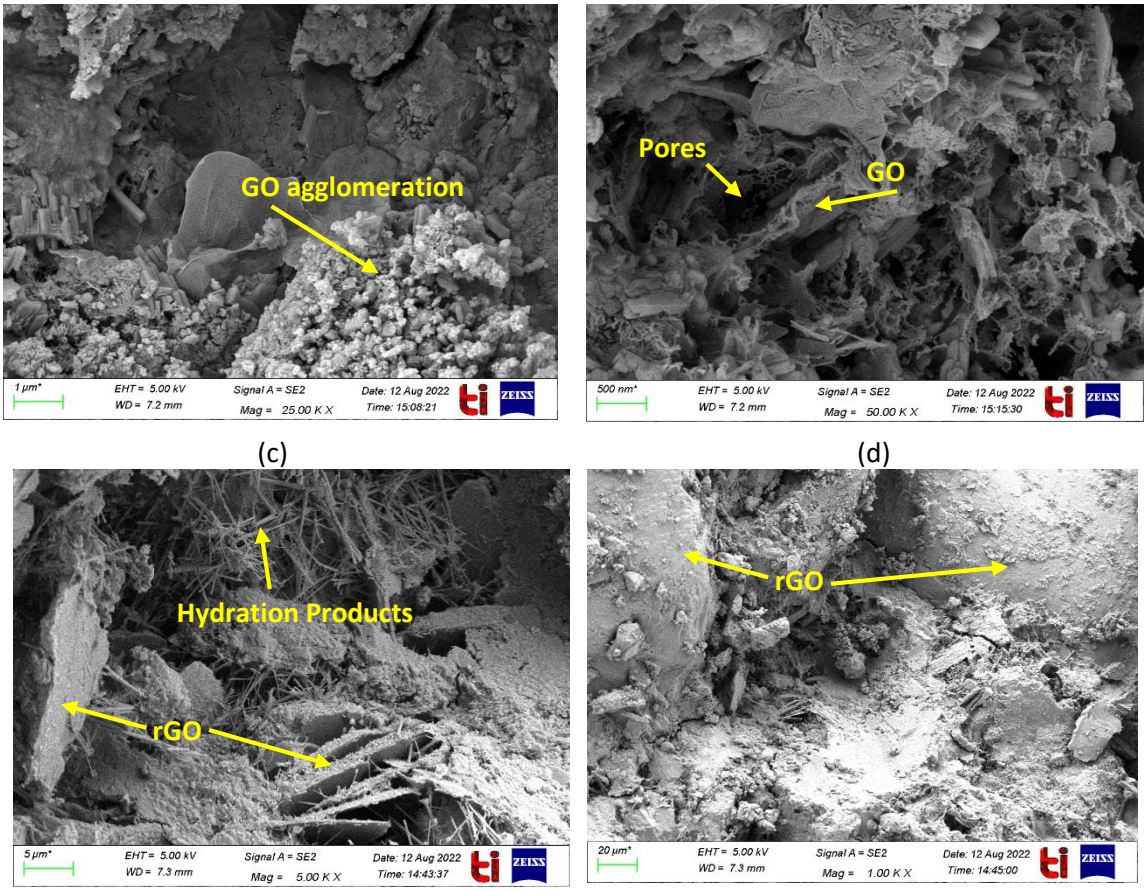

(c) (d)

(e) (f)

Figure 4.25 SEM images of (a), (b) Control Specimens (c), (d) GO-M1 cementitious composites (e), (f) rGO-M1 cementitious composites

4.7 SUMMARY

For same percentage of addition of GO and rGO i.e., in case of GO-M1 and rGO-M3 mix, GO showed more strength. Though comparing with the best mixes of GO and rGO i.e., GO-M1 and rGO-M1 mix, both GO-M1 mix achieved slightly higher compressive strength than rGO specimens. Despite of rGO stronger physical properties, random pore filling nature of rGO resulted in slightly lower flexural strength compared to GO mixes (Qureshi and Paneshar 2019). Though the difference is not significant.

On addition of GO and rGO at all addition percentages, FCR decreases on increasing the load, corresponding to increase in electrical conductivity and comes back to its original value after sample failure in monotonic loading, corresponding to decrease in conductivity. Thus, overall pattern of piezoresistive behaviour is followed. Piezoresistivity is dependent on the number of contact points and conductive passage in the cement matrix. This creates a tunnelling effect allowing continuous migration of electrons (Zai et al. 2021). it can be observed that rGO-M1 mix achieved the maximum sensitivity, followed by GO-M3 mix, indicating maximum contact

points are formed in rGO-M1 mix leading to enhanced piezoresistive behaviour. The reduces sensitivity of higher dosage of rGO mixes, might be possibly due to agglomeration of rGO at higher dosage.

CHAPTER 5
CONCLUSIONS

5.1 GENERAL

The results of the present study involving the addition of GO and rGO in cement-based composites for various mechanical and piezoresistive properties can be concluded as following:

1) Both GO and rGO increased the compressive strength of the cementitious mortar at 28 days and 56 days.
2) In comparison with the control specimen, the compressive strength of 0.1%, 0.2% and 0.3% addition of GO increased by 13.4%, 6.6% and 7.6% respectively at 28 days and 17.4%, 4.1% and -14.3% respectively at 56 days.
3) In comparison with the control specimen, the compressive strength of 0.06%, 0.08% and 0.1% addition of rGO increased by 59.6%, 53.8% and 40% respectively at 7 days. However only 2% increase in strength is observed at 56 days for 0.08% addition of rGO. This increase in strength is mainly attributed to high physical strength of rGO.
4) For GO, with an increase in the percentage of GO, flexural strength also increased. The maximum strength is achieved for GO-M3 mix, which showed 27% increase in flexural strength compared to control mix at 28 days and 10% increase at 56 days.
5) In case of rGO, maximum increase of 27% in flexural strength is observed for rGO-M1 mix with 0.06% addition of rGO, followed by 21% for rGO-M2 mix and 8.5% of rGO-M3 mix at 28 days.
6) For same percentage of addition of GO and rGO i.e., in case of GO-M1 and rGO-M3 mix, GO showed more strength. Though comparing with the best mixes of GO and rGO i.e., GO-M1 and rGO-M1 mix, both GO-M1 mix achieved slightly higher compressive strength than rGO specimens.
7) The main reason for decrease in compressive strength at higher dosage of GO is poor dispersion of GO in the cement matrix, leading to agglomeration. This is mainly attributed to presence of high content of functional groups in GO, which chemically binds with cement hydration products leading to increased strength and pore filling mechanism. Despite of rGO stronger physical properties, random pore filling nature of rGO resulted in slightly lower flexural strength compared to GO mixes.
8) It was found that for control specimens, on increasing the stress, no significant change in FCR values were observed at both 28 days and 56 days.

9) On addition of GO and rGO at all addition percentages, FCR decreases on increasing the load, corresponding to increase in electrical conductivity and comes back to its original value after sample failure in monotonic loading, corresponding to decrease in conductivity. Thus, overall pattern of piezoresistive behaviour is followed.
10) It was found that rGO-M1 mix achieved the maximum sensitivity, followed by GO-M3 mix, indicating maximum contact points are formed in rGO-M1 mix leading to enhanced piezoresistive behaviour. The reduced sensitivity of higher dosage of rGO mixes, might be possibly due to agglomeration of rGO at higher dosage.
11) The mechanism behind the piezoresistive behaviour of the GO and rGO composite is that when compressive load is applied the distance between the GO and rGO sheet is reduced and conductive paths are formed. This leads to increased conductivity and change in FCR.
12) It was observed that microstructure of cementitious mortar got densified by addition of 0.1% GO and 0.06% rGO. This confirmed the pore filling nature of the composites.
13) Compared to GO, in rGO specimens, cluster of rGO is more randomly distributed, this is attributed to lower surface area of rGO, compared to GO. Thus, denser microstructure was observed in rGO-M1 mix compared to control, which indicates micro-crack bridging.
14) The piezoresistive performance of cementitious composites with GO and rGO confirms their ability to become intrinsic cement-based sensors.

5.2 FUTURE SCOPE

1) Effect of the external environment such as temperature, carbon dioxide, chloride content, and humidity on the sensing performance cementitious composite with GO and rGO needs to be further explored.
2) This study limits piezoresistive performance for monotonic loading only. However, considering the real-life conditions, performance of developed SSC needs to be explored under cyclic loading to understand its repeatability.
3) More detailed microstructural analysis needs to be performed to understand mechanism behind piezoresistive performance of GO and rGO based SSC.
4) Due to inaccurate results obtained for electrical resistivity tests in the present study, the test needs to be repeated with smaller embedded steel plates.
5) Alternative way of inducing piezoresistive behaviour in terms of sensors using GO and rGO need to be studied.

6) Potential application or corrosion Application of SSC for other areas such as corrosion monitoring and crack detection are other potential applications in the construction industry that need to be discovered.

REFERENCES

A. Mohammed, J. Sanjayan, W. Duan, A. Nazari, Graphene Oxide Impact on Hardened Cement Expressed in Enhanced Freeze–Thaw Resistance, Journal of Materials in Civil Engineering 28(9) (2016) 04016072.

Azhari, F., & Banthia, N. (2012). Cement-based sensors with carbon fibers and carbon nanotubes for piezoresistive sensing. Cement and Concrete Composites, 34(7), 866–873. https://doi.org/10.1016/j.cemconcomp.2012.04.007

Chung, D. D. L. (2016). Piezoresistive Cement-Based Materials for Strain Sensing. Journal of Intelligent Material Systems and Structures, *13*(9), 599–609. https://doi.org/10.1106/104538902031861

H. Du, S. Dai Pang, Enhancement of barrier properties of cement mortar with graphene nanoplatelet, Cement and Concrete Research 76 (2015) 10-19.

Han, B.; Yu, X.; Ou, J. Sensing Mechanisms of Self-Sensing Concrete. Self-Sensing Concrete in Smart Structures; Elsevier: Amsterdam, The Netherlands, 2014; p. 163–187, https://doi.org/10.1016/B978-0-12-800517-0.00006-X.

Haining Luo Thesis- A Theoretical Study of Graphene Oxide Chemical Structure, The University of Queensland, The School of Mechanical and Mining Engineering 2017.

J. Tao, X. Wang, Z. Wang, Q. Zeng, Graphene nanoplatelets as an effective additive to tune the microstructures and piezoresistive properties of cement-based composites, Construction and Building Materials 209 (2019) 665-678.

Jin Tao, Xiaohu Wang, Zhendi Wang, Qiang Zeng, Graphene nanoplatelets as an effective additive to tune the microstructures and piezoresistive properties of cement-based composites/Construction and Building Materials 209 (2019) 665–678 https://doi.org/10.1016/j.conbuildmat.2019.03.173

K. Parvez, Z.-S. Wu, R. Li, X. Liu, R. Graf, X. Feng, K. Mullen, Exfoliation of graphite into graphene in aqueous solutions of inorganic salts, Journal of the American Chemical Society 136(16) (2014) 6083-6091.

L. Zhao, X. Guo, L. Song, Y. Song, G. Dai, J. Liu, An intensive review on the role of graphene oxide in cement-based materials, Construction and Building Materials 241 (2020) 117939.

M. Murugan, M. Santhanam, S.S. Gupta, T. Pradeep, S.P. Shah, Influence of 2D rGO nanosheets on the properties of OPC paste, Cement and Concrete Composites 70 (2016) 48 59.

M.V. Kiamahalleh, A. Gholampour, D.N.H. Tran, T. Ozbakkaloglu, D. Losic, Physiochemical and mechanical properties of reduced graphene oxide–cement mortar composites: Effect of reduced graphene oxide particle size, Construction and Building Materials 250 (2020) 118832.

Madbouly, A.I., Mokhtar, M.M. and Morsy, M.S. (2020), "Evaluating the performance of rGO/cement composites for SHM applications", Construction and Building Materials, 250, p.118841.

Papanikolaou, C. Litina, A. Zomorodian, et al., Effect of natural graphite fineness on the performance and electrical conductivity of cement paste mixes for self- sensing structures, Materials 13 (24) (2020) 5833.

Q. Wang, J. Wang, C. Lu, B. Liu, K. Zhang, C. Li, Influence of graphene oxide additions on the microstructure and mechanical strength of cement, New Carbon Materials 30(4) (2015) 349-356.

Q. Yang, P. Liu, Z. Ge, et al., Self-sensing carbon nanotube-cement composite material for structural health monitoring of pavements, J. Test. Eval. 48 (3) (2020) (20190170).

Qureshi, T.S. and Panesar, D.K. (2019), "Impact of graphene oxide and highly reduced graphene oxide on cement-based composites", Construction and Building Materials, 206, pp.71-83.

R. Raccichini, A. Varzi, S. Passerini, and B. Scrosati, "The role of graphene for electrochemical energy storage," Nature Materials, vol. 14, pp. 271-279, Mar 2015.

Reza, F.; A Yamamuro, J.; Batson, G.B. Electrical resistance change in compact tension specimens of carbon fiber cement composites. Cem. Concr. Compos. **2004**, *26*, 873–881, doi:10.1016/j.cemconcomp.2003.06.002.

S. Lv, S. Ting, J. Liu, Q. Zhou, Use of graphene oxide nanosheets to regulate the microstructure of hardened cement paste to increase its strength and toughness, CrystEngComm16(36) (2014) 8508-8516.

W. Dong, W. Li, X. Zhu, et al., Multifunctional cementitious composites with integrated self-sensing and hydrophobic capacity for structural health monitoring, Cem. Concr. Compos. (2021) 103962.

W. S. Koh, C. H. Gan, W. K. Phua, Y. A. Akimov, and P. Bai, "The Potential of Graphene as an ITO Replacement in Organic Solar Cells: An Optical Perspective," Ieee Journal of Selected Topics in Quantum Electronics, vol. 20, Jan-Feb 2014.

Zhai, S., Pang, B., Liu, G., Zhang, Y., Xu, K., She, W. and Zhang, Y. (2021), “Investigation on preparation and multifunctionality of reduced graphene oxide cement mortar”, Construction and Building Materials, 275, p.122119.

Z. Pan, L. He, L. Qiu, A.H. Korayem, G. Li, J.W. Zhu, F. Collins, D. Li, W.H. Duan, M.C. Wang, Mechanical properties and microstructure of a graphene oxide–cement composite, Cement and Concrete Composites 58 (2015) 140-147.

Ouriginal by Turnitin

Document Information

Analyzed document	Analysis of self sensing capability of GO and rGO based cementitiouscomposites.docx (D143380682)
Submitted	2022-08-30 07:43:00
Submitted by	Arpit Goyal
Submitter email	arpit.goyal@thapar.edu
Similarity	0%
Analysis address	arpit.goyal.thapar@analysis.urkund.com

Sources included in the report

SA **Delhi Technological University, New Delhi / NANO CONCRETE report.pdf** 1
Document NANO CONCRETE report.pdf (D24353877)
Submitted by: anandkrv1992@gmail.com
Receiver: ramakant.shukla.dtu@analysis.urkund.com

SA **PSG College of Technology / et project1.docx** 1
Document et project1.docx (D51878443)
Submitted by: spk.civil@psgtech.ac.in
Receiver: spk.civil.psgcot@analysis.urkund.com

SA **Dr. B. R. Ambedkar National Institute Of T / CHAPTER 3-5.docx** 1
Document CHAPTER 3-5.docx (D99004414)
Submitted by: kothiyalnc@nitj.ac.in
Receiver: kothiyalnc.nitj@analysis.urkund.com